GEAP-4310
JULY, 1963

ACCENT ON VALUE

GENERAL AND LOCALIZED CORROSION STUDIES OF TYPE 300 SERIES AUSTENITIC STAINLESS STEELS IN SIMULATED SUPERHEAT REACTOR ENVIRONMENT

By
W.L. PEARL
G.G. GAUL
G.P. WOZADLO

U.S. ATOMIC ENERGY COMMISSION
CONTRACT AT(04-3)-189
PROJECT AGREEMENT 13

ATOMIC POWER EQUIPMENT DEPARTMENT
GENERAL ELECTRIC
SAN JOSE, CALIFORNIA

DISCLAIMER

GEAP-4310
July 1963

GENERAL AND LOCALIZED CORROSION STUDIES OF TYPE 300 SERIES AUSTENITIC STAINLESS STEELS IN SIMULATED SUPERHEAT REACTOR ENVIRONMENT

by

W. L. Pearl
G. G. Gaul
G. P. Wozadlo

Prepared For The

United States Atomic Energy Commission
Under Contract AT(04-3)-189
Project Agreement No. 13

ATOMIC POWER EQUIPMENT DEPARTMENT
GENERAL ELECTRIC
SAN JOSE, CALIFORNIA

APPROVED:

W. L. Fiock, Project Engineer
Nuclear Superheat Project

S. Naymark, Manager
Fuels and Materials Development

LEGAL NOTICE

This report was prepared as an account of Government sponsored work. Neither the United States, nor the Commission, nor any person acting on behalf of the Commission:

A. Makes any warranty or representation, expressed or implied, with respect to the accuracy, completeness, or usefulness of the information contained in this report, or that the use of any information, apparatus, method, or process disclosed in this report may not infringe privately owned rights; or

B. Assumes any liabilities with respect to the use of, or for damages resulting from the use of any information, apparatus, method, or process disclosed in this report.

As used in the above, "person acting on behalf of the Commission" includes any employee or contractor of the Commission, or employee of such contractor, to the extent that such employee or contractor of the Commission, or employee of such contractor prepares, disseminates, or provides access to, any information pursuant to his employment or contract with the Commission, or his employment with such contractor.

TABLE OF CONTENTS

LIST OF FIGURES

LIST OF FIGURES (Continued)

LIST OF TABLES

INTRODUCTION

The 300 series stainless steels had been selected originally as the reference fuel cladding material for utilization in several superheat reactor (SHR) systems being designed and built. Subsequently, fuel jacket failures occurred in Type 304 stainless clad fuel elements exposed in the Vallecitos boiling water reactor (BWR) superheated steam loop (SADE)[1,2] and later out-of-pile stress corrosion tests.[3] Because of the questionable dependability of such commercial grades of stainless steel other commercially available materials were considered for this SHR fuel cladding application.

Based on the work of others[4] the high-nickel alloys were considered of significant promise to justify a major evaluation program. The favorable results of said evaluation program carried out with Inconel, Incoloy, and Hastelloy-X in the out-of-pile superheat facilities have been summarized.[5]

Because of the excellent superheat corrosion resistance of the austenitic stainless steels in general, and their lower neutron cross section than the high-nickel alloys, the possibility of the further use of 300 series stainless steels for cladding superheat fuel elements was considered. Since most of the cladding failures experienced in the SADE exposures were intergranular in nature[1,2] the respective proponents hoped that the stabilized Type 348 stainless steel (SS) or the low-carbon Type 316 SS might avoid such intergranular attack by minimizing the tendency to sensitize.[6]

Several investigators[7,8] have found that stainless steels containing 20 percent nickel prepared by vacuum melting consistently resist cracking at high stress levels in an aggressive medium as magnesium chloride solutions. The removal of the nitrogen in particular was found to be beneficial in decreasing the susceptibility to attack.

The out-of-pile evaluation program of the high nickel alloys[5] was expanded to include a general evaluation of the austenitics committed for SHR applications and some austenitics specially prepared by vacuum melting to lower the contained nitrogen contents to a minimum.

It is the purpose of this report to summarize the results of the general and stress corrosion studies carried out to date on several 300 series stainless steels in the out-of-pile superheat facilities as part of Task E of the Atomic Energy Commission sponsored Superheat Program, Contract AT(04-3)-189, Project Agreement No. 13. It is the additional purpose to summarize several equipment failures that have contributed substantially to the understanding of the 300 series stainless steels performance in SHR simulated superheated steam.

CONCLUSIONS

The following conclusions are based on the out-of-pile general corrosion and localized attack studies completed to-date on several 300 series stainless steels:

1. Utilizing a sodium chloride-cycle test that produces a type failure that can occur in a superheat reactor system, Types 347 and vacuum-melted 304 SS have failed while vacuum-melted 310 SS was acceptable.

2. An improved chloride cycle test utilizing ferric chloride as the additive has been developed that produces an intergranular type failure similar to that experienced in the fuel cladding failures in the SADE and ESADE facilities. Types 304 and 316 SS have failed in the test.

3. Present methods of ultrasonic testing will find through cracks but are not completely dependable for assessing lesser degrees of intergranular attack.

4. It is hypothesized that a definite interplay exists between chemical attack and stress. The application of stress will orient intergranular attack preferentially in a direction perpendicular to the stress.

MATERIALS

The heat transfer specimens consisted of tubes either welded or seamless, cold drawn, annealed, and pickled. Each test sheath was 36 3/4-inches long by 9/16-inch OD by 0.500-inch ID. The ends of the sheaths were machined to 0.560-inch OD and the last 1/4 inch on each end threaded. The sheaths were marked, degreased in acetone, pickled for one-half hour in a 130 F, 20 percent, nitric acid bath, washed, dried, and weighed.

For the localized corrosion tests (cycle tests) the sheaths were heated as specified in a tube furnace utilizing a flowing argon environment. The heat-treated sheaths were descaled in a solution of 20 percent sodium hydroxide and 3 percent potassium permanganate, scrubbed with soap and water, rinsed and acetone dried prior to the pickling procedure.

The low nitrogen materials were fabricated into tubing by Nuclear Metals, Inc., West Concord, Massachusetts, from vacuum-melted ingots supplied by the General Electric Research Laboratory, Schenectady, New York. The other materials were obtained commercially to standard ASTM specifications.

The chemical composition and mechanical properties of the test materials are listed in Table I. The Type 347 SS as-received also meets the ASTM specifications for Type 348 SS.

After test and prior to descaling, the tubes and test coupons were weighed and examined at magnifications up to 40X by means of a stereo-microscope. Descaling, as required, was performed in a solution of 20 percent sodium hydroxide and 3 percent potassium permanganate operated at 210 F up to 1-1/2 hours. Nylon brushes and nylon wool were used to remove the rotted scale. Control pieces gave less than two mg/dm^2 loss of base metal in the same time. The specimens were weighed as required. For some tests, the sheaths were examined by ultrasonics for flaw indications greater than the normal level present in incoming tubing. The sheaths and coupons were sectioned in selected areas for microscopic examination.

TABLE I

COMPOSITION OF 300 SERIES STAINLESS STEELS

Chemical Composition	Steel Code	Commercial 304 Y	Commercial 316 WC	Commercial 347 XB	Commercial 347 X	Vacuum Melted 304 YC	Vacuum Melted 304 YB	Vacuum Melted 310 WB	Vacuum Melted 310 WD
C		0.05	0.06	0.05	0.06	0.012	0.067	0.01	0.24
Mn		1.08	1.77	1.58	1.64	1.33	1.16	1.31	1.72
P		0.016	0.017	0.020	0.023	<0.01	<0.01	<0.01	0.01
S		0.006	0.008	0.016	0.018	0.008	0.007	0.008	0.008
Si		0.73	0.73	0.43	0.68	0.98	1.06	1.06	1.06
Ni		9.32	12.54	10.70	10.54	9.92	9.93	20.6	20.5
Cr		18.52	17.37	18.84	18.88	19.8	19.6	25.3	25.0
Mo			2.72	0.26	0.20				
Ta				0.03	0.09				
Cb				0.70	0.50				
Cu				0.25	0.19				
N_2						0.0064	0.0059	0.0082	0.0075
Mechanical Properties									
Tensile strength, psi		92,800		91,400	95,750	84,500	88,200	78,500	99,100
Yield strength, psi		36,500		42,500	42,100	33,100	32,200	33,100	47,000
Elongation in 2 inches, %		60		47	49				

GENERAL CORROSION

A. Method

The general corrosion tests were carried out in the CL-1 superheat corrosion facility, shown in schematic diagram in Figure 1 and previously described elsewhere.[9, 10] The tests with heat transfer were performed with longitudinal stresses applied when indicated, as described for stress testing of Type 304 stainless steel.[3] The runs for each material approximated 1000 hours. The facility water was maintained at neutral pH with no chemical additives. The water resistivity was maintained above 2 megohm-centimeters during the test runs with chloride maintained below 0.05 ppm. Oxygen and hydrogen were maintained in the water to result in a level in the steam typical of quantities generated radiolytically in a BWR system. The facility operating conditions during the general corrosion test runs are summarized in Table II. The test with Type 316 SS was carried out in the exit superheater position only.

B. Results

The descaled weight losses and the calculated metal-to-system losses are summarized in Table III. The Type 304 stainless steel values reported previously[10] are shown for comparison purposes.

Almost complete spalling of the scale with a correspondingly high metal-to-system loss in the 1200-1300 F temperature range occurred on the Type 316 SS at the stresses that the Type 310 SS (LCVM) and Type 304 SS[3] had performed acceptably. Figure 2 shows sections of the Type 316 SS test sheath exposed at metal temperatures of 1100 F and 1300 F.

The Type 347 SS, which had no applied stress, performed acceptably in general corrosion but had some intergranular attack indicated in the 1100-1300 F range as seen in Figure 3. The positive numbers indicated in Table III for metal to system loss in the 800-1100 F range probably result from some deposition on the sheaths from the flowing steam with little to no oxide lost to the system.

The Type 310 SS (LCVM) showed no evidence of localized attack. A compositionally disturbed layer as seen previously with Type 304 SS[10] and the high nickel alloys[5] was found on the 1300 F Type 310 SS specimen to an average depth of 0.5 mils, see Figure 4.

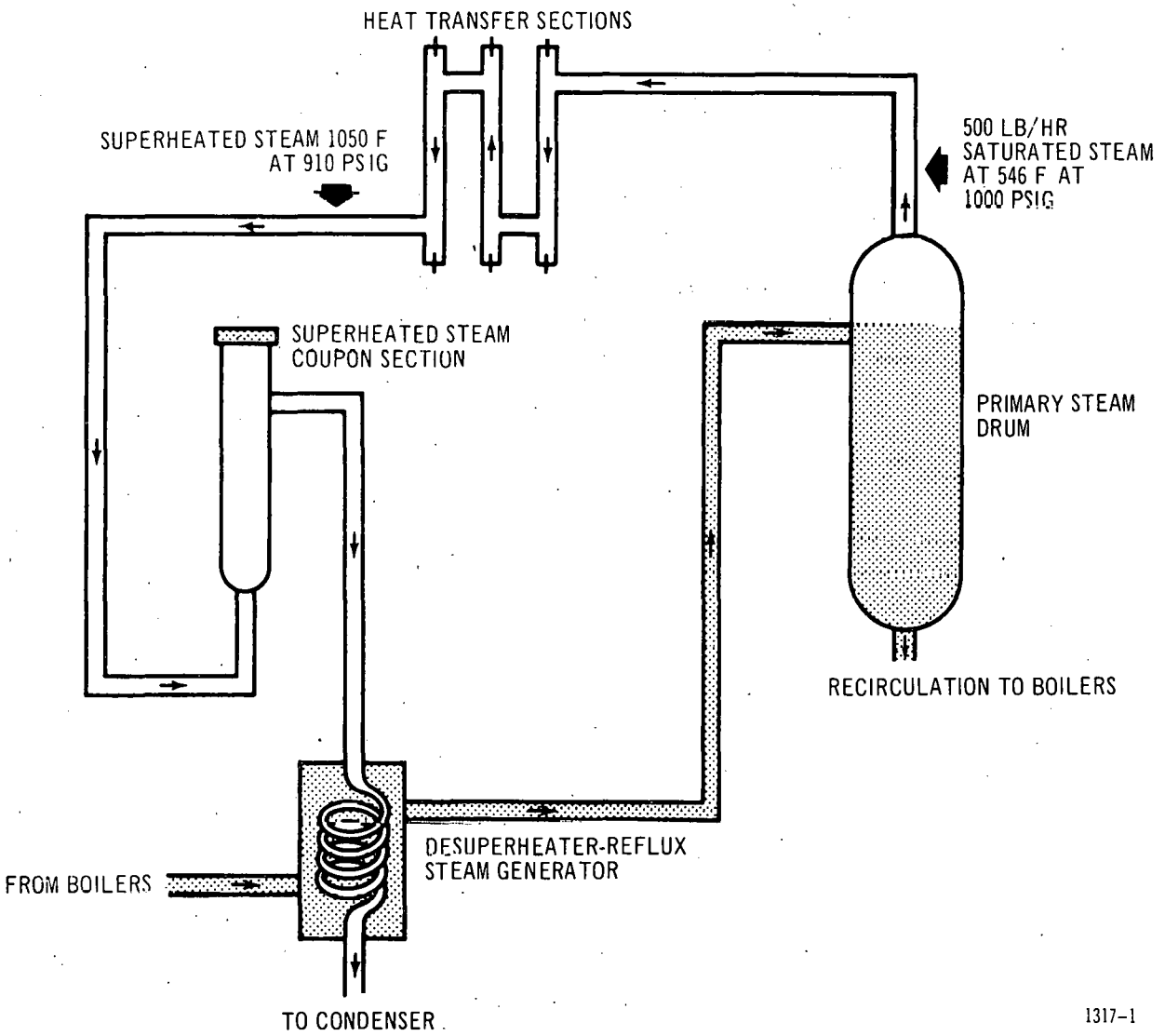

Figure 1. Superheat Corrosion Facility

TABLE II

OPERATING CONDITIONS GENERAL CORROSION TESTS

Steel Under Test	347	310 (LCVM)	316
Code	X	WB	WC
Run No.	48	59	60
Length of Test, hr	1016	997	895
Steam Flow, lb/hr	462	444	427
Moisture in Inlet Steam, %	~ 1	~ 1	~ 1
Steam Temperatures, °F			
Inlet	546	546	N/A
Outlet of entrance heater	656	656	N/A
Outlet of middle heater	842	845	830
Outlet of exit heater	1044	1047	1049
Inlet Steam Gas Content			
Oxygen, ppm (range)	12.5-25.0	17.39-27.7	16.0-24.0
(mean)	17.2	19.5	20.7
Hydrogen, ppm (range)	1.4-6.3	2.1-3.9	2.0-3.0
(mean)	2.3	2.8	2.8
Average Heat Flux, Btu/hr-ft^2			
Entrance heater	165,000	159,000	N/A
Middle heater	169,000	164,000	N/A
Exit heater	174,000	168,000	179,000
Applied Stresses, psi			
Entrance sheath	None	25,000	N/A
Middle sheath	None	14,000	N/A
Exit sheath	None	7,000	7,000

Calculated Metal Temperatures (all runs)

Entrance sheath	800-900° F
Middle sheath	900-1100° F
Exit sheath	1100-1300° F

TABLE III

CORROSION WITH HEAT TRANSFER IN SUPERHEATED STEAM

Stainless Steel Type	Code	Calculated Metal Temperature °F	Time Hours	Descaled Weight Loss mg/dm^2	Metal-to-System Loss* mg/dm^2
310	WB	1100-1300	997	126	57
316	WC	1100-1300	895	1005	419
347	XB	1100-1300	1000	488	13
		900-1100	1000	54	+1**
		800- 900	1000	24	+2**
304		1100-1300	950	452	120
		1100-1300	1032	284	62
		900-1100	950	143	9
		800- 900	950	12	10

* Corrosion scale assumed to be 72% metal.

** Weight gain.

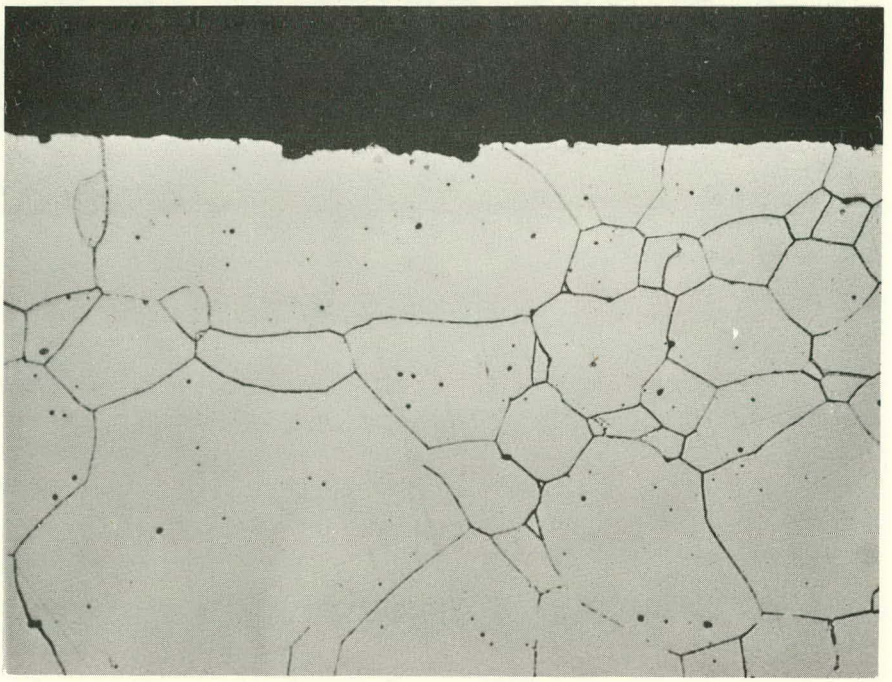

a. Calculated Metal Temperature - 1100 F

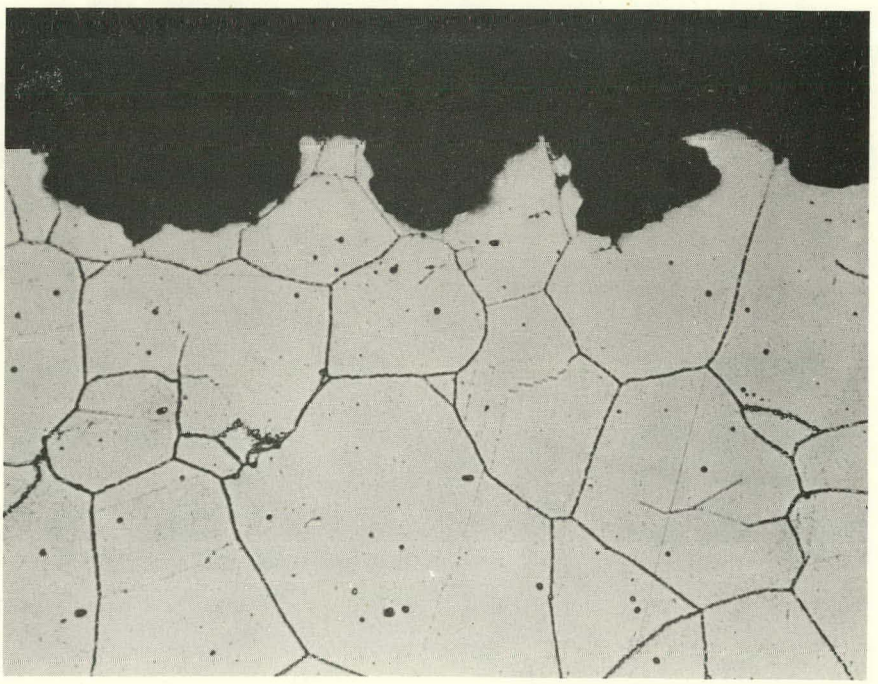

b. Calculated Metal Temperature - 1300 F

Figure 2. Type 316 SS, Heat Transfer Specimens, 895 Hours
Descaled Glyceregia Etch 500X

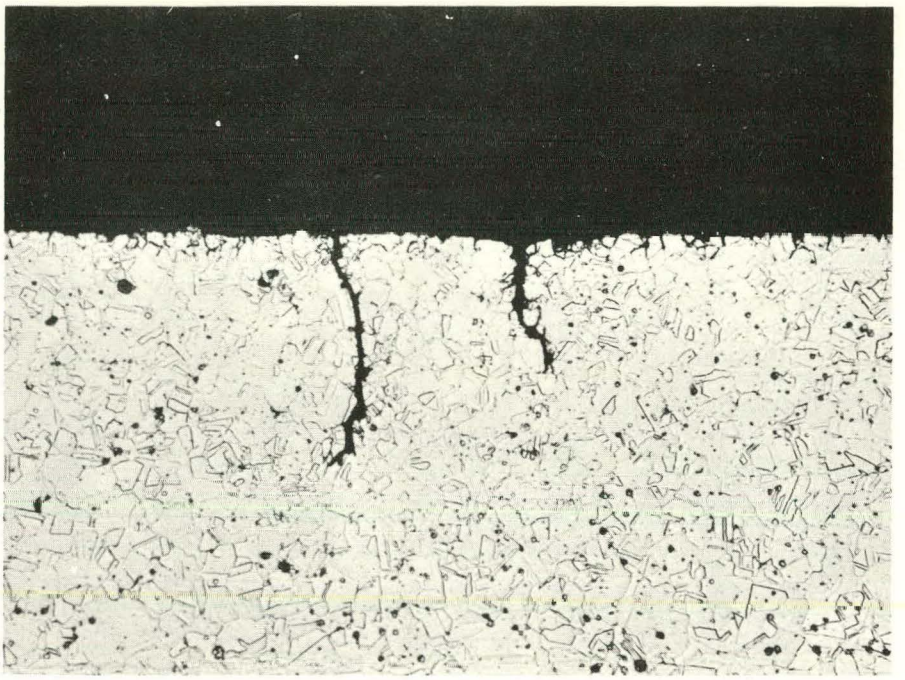

Figure 3. Type 347 SS Heat Transfer Specimen, 1016 Hours
Calculated Metal Temperature 1300 F
Descaled 60% Nitric Acid Etch 500X

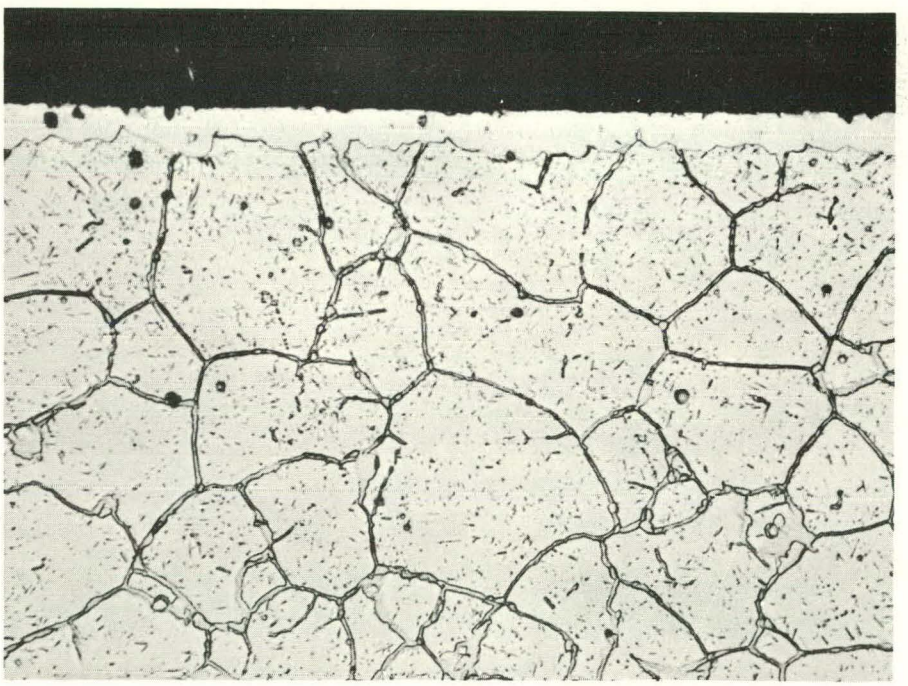

Figure 4. Type 310SS (LCVM) Heat Transfer Specimen, 997 Hours
Calculated Metal Temperature 1300 F Descaled
10% Oxalic Acid - Electrolytic Etch 500X

LOCALIZED ATTACK - SODIUM CHLORIDE CYCLE

The first fuel jacket failure that occurred in the Type 304 stainless clad fuel element exposed in SADE was attributed to chloride stress corrosion cracking.[1] The source of the problem was indicated as a combination of abnormally high water seepage from the BWR into SADE and abnormally high chloride ion concentration in the VBWR coolant. The SADE fuel element during this time was exposed to saturated steam at varying temperatures (with corresponding varying saturation pressures) part of the time. With little to no superheat being generated by the fuel, a large percentage of the total surface area of the fuel could become wetted during this period by moisture carryover with the VBWR steam.

A cycle run was developed[3] to approximate the myriad of wetting and low superheat cycles experienced in SADE with chloride added as sodium chloride to the recirculating water. Failure of Type 304 SS was obtained in periods less than two weeks. The failures were predominantly transgranular in nature with some intergranular attack at the higher temperatures.[3]

The so-called sodium chloride (NaCl) cycle has been used as a screening test recognizing that the type failures produced can occur in a SHR system but does not reproduce the most general type failure experienced in the fuel cladding exposures in the SADE facility.

A. Method

The CL-1 and CL-4 superheat facilities, represented by the schematic diagram shown in Figure 1, were utilized for carrying out the localized corrosion evaluations.

The cycle run operation of the CL-4 facility was similar to a corresponding run in the CL-1 facility with one major exception. Operation at a low pressure of approximately 100 psig and low superheat resulted in a much higher liquid carryover as determined by heat balance measurements. Also, the amount of carryover cycled so that the actual point of initiation of superheating varied on the heaters with the net effect of spreading the solids deposit over a larger portion of the 3-sheath assembly and allowing moisture to come in contact with previous deposits. In all cases for both facilities the steam leaving the exit sheath was superheated.

The operating conditions were modified to utilize a two-week total cycle. Oxygen and hydrogen were maintained in the water at the same level utilized for general corrosion testing, but the chloride level in the recirculating water was raised to about 1.5 ppm added as sodium chloride. The facility operating conditions during the cycling test runs are summarized in Table IV.

TABLE IV

OPERATING CONDITIONS NaCl CYCLING TESTS

Steel	304[1]	304[1]	347	304 (LCVM)	310 (LCVM)	304[2] (HCVM)
Code	Y	Y	XB	YL	WB	YB
CL FACILITY UTILIZED	1	4	1	4	4	4
Run Number	53	26	55	30	31	32
Total Elapsed Time, Hours	324	114	327	343	318	113
Step One						
Elapsed Time, Hours	114	114	91	98	88	90
Steam Temp.,°F Inlet of Entrance Heater	352	365	350	350	350	351
Outlet of Exit Heater	362	388	360	383	360	367
Step Two						
Elapsed Time, Hours	97		73	64	72	23
Steam Temp.,°F Inlet of Entrance Heater	546		546	546	546	548
Outlet of Exit Heater	550		549	551	557	557
Step Three						
Elapsed Time, Hours	40		50	62	47	
Steam Temp.,°F Inlet of Entrance Heater	547		546	546	546	
Outlet of Exit Heater	1050		1043	1047	1045	
Step Four						
Elapsed Time, Hours	71		70	73	66	
Steam Temp.,°F Inlet of Entrance Heater	353		353	350	350	
Outlet of Exit Heater	362		361	369	372	
Step Five						
Elapsed Time, Hours	2		43	46	45	
Steam Temp.,°F Inlet of Entrance Heater			546	546	546	
Outlet of Exit Heater			549	1040	1037	
Applied Stresses, Low Superheat, psi						
Entrance Sheath	25,000	25,000	25,000	25,000	25,000 to 17,000[3]	22,500
Middle Sheath	25,000	25,000	25,000	25,000	25,000 to 18,200	22,500
Exit Sheath	25,000	25,000	25,000	25,000	25,000 to 17,000	22,500
Applied Stresses, Full Superheat, psi						
Entrance Sheath	25,000		25,000	25,000	19,000 to 25,000[4]	
Middle Sheath	14,000		14,000	14,000	8,500 to 14,000	
Exit Sheath	6,600		7,000	7,000	5,000 to 7,000	

~ 20 ppm Oxygen in steam

~ 2.5 ppm Hydrogen in steam

~ 1.5 ppm Chloride in recirculating water as NaCl

(1) Preheated for 2 hours at 1200°F.
(2) Preheated for 112 hours at 1100°F.
(3) Reduced to lower stress after 23 hours of step two for step two only.
(4) Lower stress used in step three, higher stress in step five.

B. Results

1. Type 304 (Y)

The Type 304 SS sheaths exposed to cycling tests reported previously[3] had experienced numerous transgranular cracks on the entrance sheath and some localized evidence of intergranular attack on the middle and exit sheaths. A similar test was carried out in the CL-1 superheat facility with the sheaths for the entrance and middle superheat positions heated for 2 hours at 1200 F (furnace was at temperature when pieces were inserted - air cooled) prior to insertion in the test facility. The test was terminated before the scheduled completion date because of steam leakage through the middle superheater sheath.

A residual deposit was still present on the entire lengths of the first two superheat sections with a small amount at the entrance of the exit superheater.

Figure 5 shows areas of cracking on the middle superheater with the accompanying deposit. The cracks examined, including the failures, were transgranular in nature.

The cracks found on the entrance superheater sheath were primarily transgranular although at least one showed both intergranular and transgranular in the same crack as shown in Figure 6. It is probable that intergranular cracking was also present on the middle superheater although the sections taken did not show it. Visual and ultrasonic examination of the exit sheath indicated no cracking. With the exception of the through cracks, even though many cracks were visible, not one could be identified by the dye penetrant method.

A similarly sensitized Type 304 stainless steel sheath was utilized in the middle superheater position in a later cycle run in the CL-4 facility that permitted a higher percentage of moisture carryover with the steam (15-20 percent) part of the time. The sheath failed during the first step which utilizes operation at a pressure of 150 psig and temperature of 350 F with 10 F superheat over the three position assembly. Metallurgical examination of the failed sheath showed the cracks to be transgranular.

2. Type 347 (XB)

Visual examination up to 40X showed cracks on the entrance and middle superheater sheaths but none on the exit sheath. The major residual carryover deposit was on the entrance and middle superheaters. Figure 7 is a section through a crack that is typical of those found on the sheaths and are transgranular in nature. Figure 8 indicates the type of scale appearing on the exit sheath in an area that had operated at a metal temperature of approximately 1200 F. This scale has apparently been affected by the deposited carryover material in that it is blistering and is not the normally tightly-adhering type.

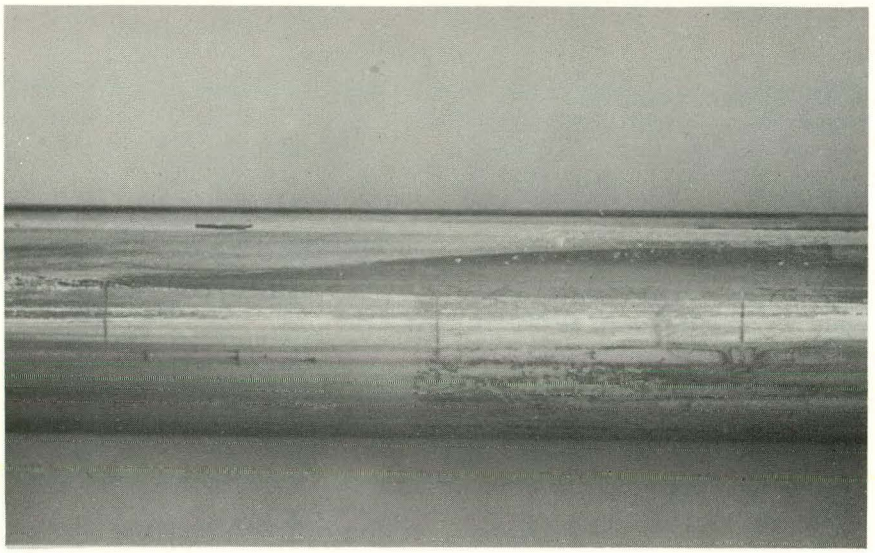

Figure 5. Type 304 SS, 324 Hours Exposure to NaCl Cycle Run Areas of Cracking on Middle Superheater Sheath Showing Varicolored Deposit

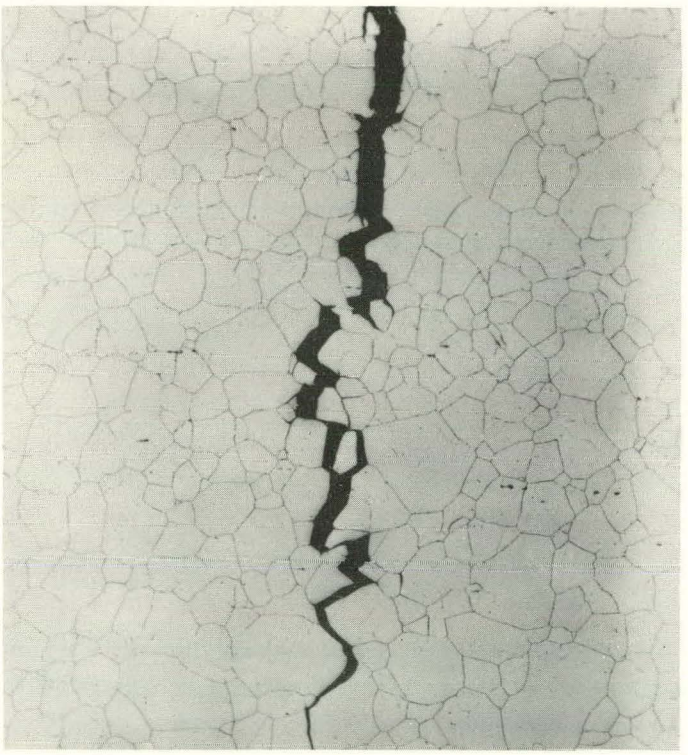

Figure 6. Type 304 SS, 324 Hours Exposure to NaCl Cycle Run Transgranular and Intergranular Attack on Entrance Superheater Sheath 10% Oxalic Acid - Electrolytic Etch 150X

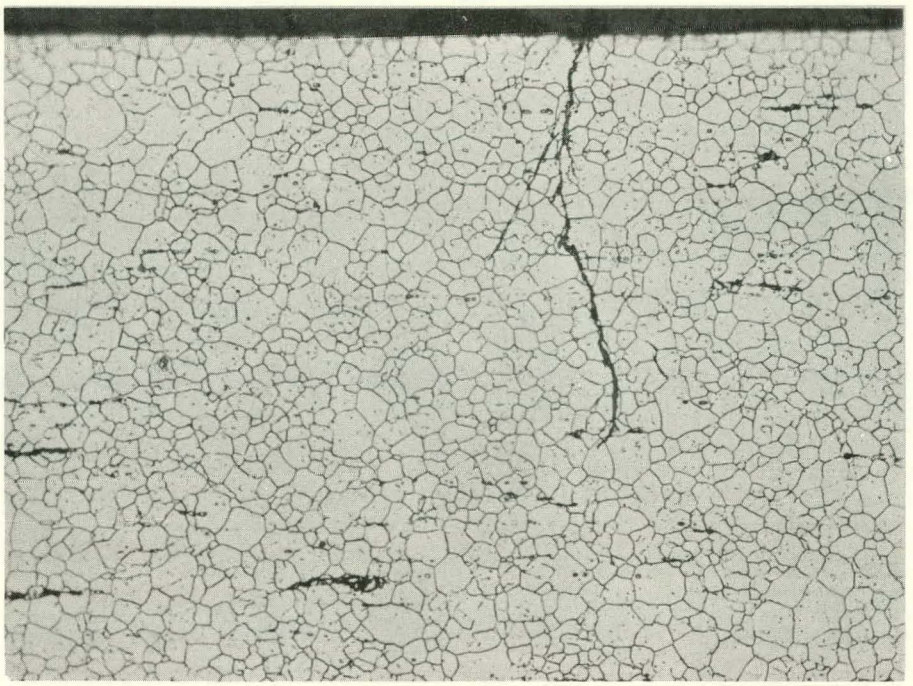

Figure 7. Type 347 SS, 327 Hours Exposure to NaCl Cycle Run
Transgranular Cracks on Middle Superheater.
60% Nitric Acid Electrolytic Etch 250X

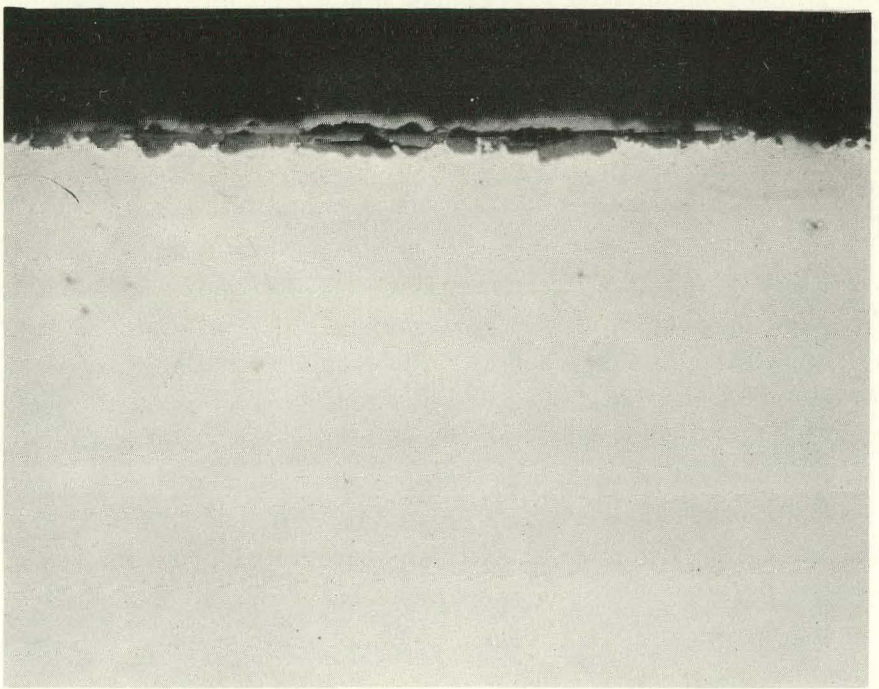

Figure 8. Type 347 SS, 327 Hours Exposure to NaCl Cycle Run
1200 F Highest Metal Temperature Unetched 500X

The exit heater indicated no suspect areas when tested ultrasonically.

3. Type 304 LCVM (YC)

Small fine transverse (perpendicular to direction of applied stress) cracks were noted by visual examination at 40X on the entrance and middle sheaths of the low carbon, low nitrogen Type 304 SS. Ultrasonic examination revealed numerous cracks in all three sheaths with the exit sheath having less than the other two. Indications were that the cracks ranged from 3 to 10 mils deep.

The microscopic examination of one cross section of the middle sheath that had been at a metal temperature of ~ 1000 F for 4 days indicated transgranular cracking as seen in Figure 9. Some sensitization is indicated.

4. Type 310 LCVM (WB)

No evidence of failure or localized attack was noted by visual or ultrasonic examination of low carbon, low nitrogen Type 310 SS exposed to the sodium chloride cycle test.

A stress of 25,000 psi, as used previously with the other austenitic stainless steels tested, was applied longitudinally to the three sheaths for the first step of the cycle. The sheaths were found to have crept during the second step so the stress was decreased by 25 percent. No further creep was noted. When taken to high temperature for step three, the stress was correspondingly decreased. The normal stresses were again applied for steps four and five with no noticeable resultant creep.

5. Type 304 HCVM (YB)

The 0.07 percent carbon, low nitrogen Type 304 SS sheaths were sensitized for 112 hours at 1100 F prior to insertion in the test. The sheath in the exit heater position failed after 63 hours while the cycle was still in the first step of 350 F steam with 10 F superheat. A nonsensitized sheath was used for a replacement and the cycle continued. The sheath in the middle heater position failed after a total of 112 hours exposure. The cycle had reached the second step of 546 F steam with 10 F superheat. Examination of both failed sheaths revealed an intergranular attack opposite the thermal sleeves in the end fittings as shown in Figure 10. The intergranular attack appeared to originate from a pit. The middle sheath was covered with pits of a few mils in depth as indicated in Figure 11. There was no evidence of cracks originating in the pits examined.

6. Additional Tests

Similar cycle tests were carried out with Type 316 SS (WC) (Run No. 33) and 0.24 percent carbon low nitrogen Type 310 SS (WD) (Run No. 34) with no cracks indicated by visual or ultrasonic examination.

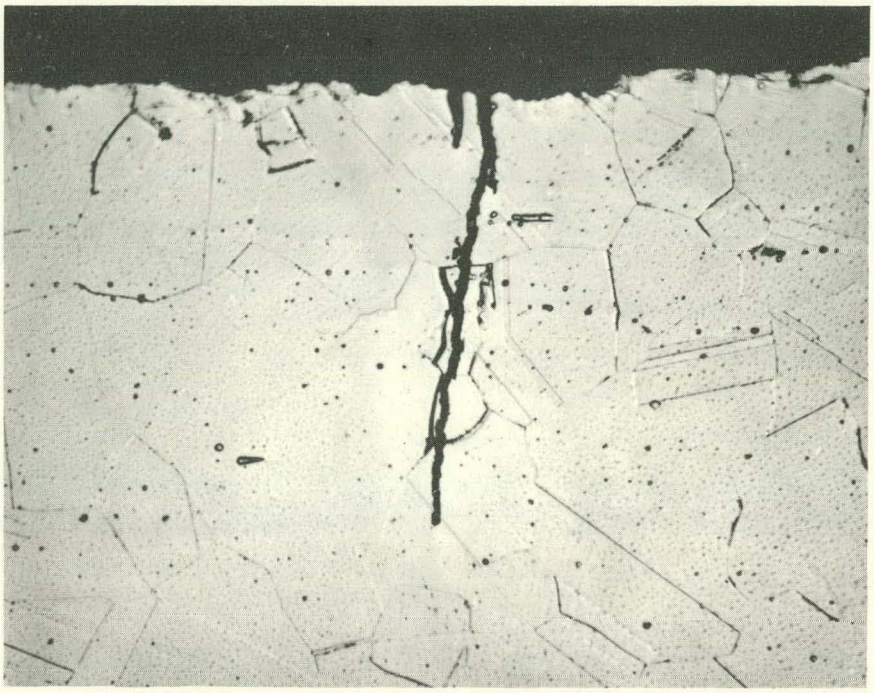

Figure 9. Type 304 SS (LCVM), 343 Hours Exposure to NaCl Cycle Run Transgranular Cracks on Middle Superheater Glyceregia Etch 500X

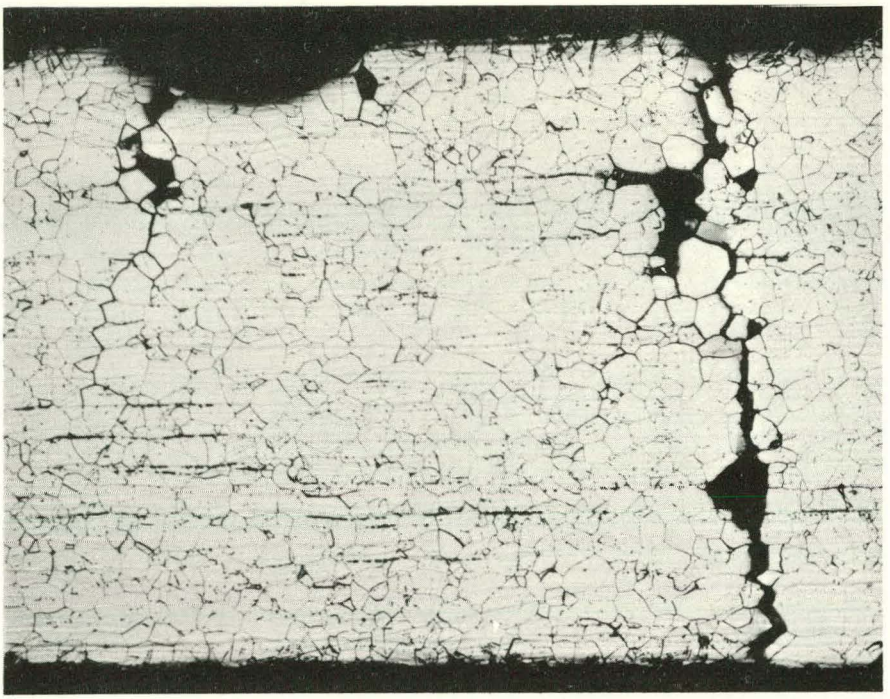

Figure 10. Type 304 SS (HCVM) 63 Hours Exposure to NaCl Cycle Run Failure Opposite Thermal Sleeve at End Fitting of Exit Superheater
10% Oxalic Acid - Electrolytic Etch 195X

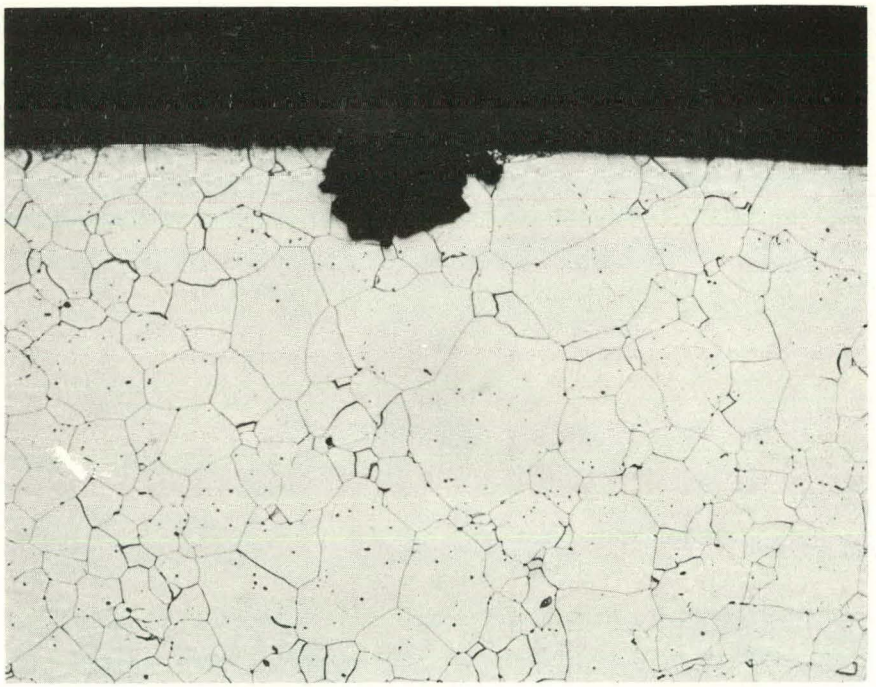

Figure 11. Type 304 SS (HCVM) 112 Hours Exposure to NaCl Cycle Run Pitting on Middle Superheater
10% Oxalic Acid - Electrolytic Etch 250X

In both cases, however, the heavy coating of carryover deposit typical of the cycle runs was not present on the sheaths. The results, therefore, could not be compared with the results of previous cycles because of the change in salt deposition pattern. The cause of the variance was later found as a cracked coil in the desuperheater-reflux steam generator permitting a portion of the flow to be bypassed. The failure is more completely detailed later (page 33).

LOCALIZED ATTACK--FERRIC CHLORIDE CYCLE

The NaCl-cycle test produced primarily a transgranular type failure that can occur in a SHR system but it did not reproduce the most general intergranular type failure experienced in the fuel cladding exposures in the SADE and more recently ESADE[11] facilities. It was recognized that the use of NaCl provided a soluble cation in the system that had not been identified in the region at or near the cracks in the superheat fuel cladding.

Some laboratory scoping tests were carried out to study the type of attack that could be expected on sensitized and unsensitized Type 304 SS and other materials of interest in the presence of the chloride salts of chromium, copper, iron, and nickel that had been identified in superheat deposits.[3, 5] Various conditions and combinations were utilized. It was generally concluded that under certain conditions that may exist in a SHR system, oxidizing chlorides (e.g., cupric chloride ($CuCl_2$) and ferric chloride ($FeCl_3$)) will attack the materials tested to varying degrees with or without the presence of high stress. Although the forms in which the chlorides exist in the carryover and resulting deposit are not known, it appeared more realistic to utilize a metallic ion that would normally be present in the BWR coolant. $FeCl_3$ was chosen as an acceptable form for a chloride and oxidizing cation additive.

Based on the increased understanding of the possible reactions involved, a development effort was undertaken to more nearly simulate the conditions that result in reactor type failures.

A. $FeCl_3$--Cycle Development

Commercial Type 304 SS (Code Y) and Type 316 SS were heat treated for 100 hours at 1100 F for use as the heater sheaths during the scoping tests. The amount of chloride added to the recirculating water was decreased to 0.1 ppm chloride added as $FeCl_3$ instead of the 1.5 ppm chloride added previously as NaCl. The experience of the scoping tests is summarized in Table V.

The two Type 304 SS sheaths that failed at the end boxes were examined metallurgically in suspect areas and found to be attacked intergranularly up to 29 mils of the 35-mil wall. The attack was found in several places originating primarily from the ID of the sheath.

It is postulated that during the no superheat part of the cycle, the failure was present and allowed steam and carryover moisture to leak through (the ID of the tube is at atmospheric pressure) and concentrate chlorides and thus cause the attack.

TABLE V

$FeCl_3$ DEVELOPMENT CYCLE RUN (No. 35)

Series No.	Steam Temperature °F Inlet	Outlet	Time, Days	Observations
1	350	370	4	See Note 1
2	546	546	Alternate days	See Note 2
	546	566	for 5 days.	
3	350	400	4	See Note 3
	546	546	1	
	546	1050	2	
	546	546	1	
4	546	600	3	See Note 4
	546*	540	1	
	546*	750	1	

All Heater Sheaths Initially 304 SS

*Chloride level increased to 0.5 ppm as $FeCl_3$.

Note 1: Visually examined three sheaths for adequacy of deposit. The inlet heater sheath was found to be failed intergranularly in the end box fitting when sheath was reinserted and pressure applied for second portion of test. The failed Type 304 SS sheath was replaced with a similarly sensitized Type 316 SS sheath. An ultrasonic test of the failed sheath indicated no other defects greater than two mils.

Note 2: Examined three heater sheaths visually at 40X and by ultrasonics. No defects reported greater than equivalent to a two mil notch. The high temperature heater sheath cracked through intergranularly in the end box fitting when sheath was reinserted and pressure applied for third portion of test. The failed Type 304 SS sheath was replaced with a similarly sensitized Type 316 SS sheath.

Note 3: Examined three heater sheaths visually at 40X and by ultrasonics. No defects reported greater than two mils. The high temperature Type 316 SS sheath was replaced with a sensitized Type 304 SS sheath.

Note 4: Three superheaters removed and dismantled for complete evaluation. Visual examination at 40X revealed some cracking on inlet sheath while all three sheaths indicated no defect greater than two mils when tested by ultrasonics.

The three sheaths removed at the end of the fourth series were examined. Intergranular attack was found on the entrance Type 316 SS sheath up to 10-mils deep originating on the OD as shown in Figure 12 and on the middle Type 304 SS sheath nearly through the wall originating from the ID, Figure 13. Intergranular attack was also noted on the exit sheath.

It had been anticipated that any intergranular attack experienced could be easily identified by ultrasonic tests. As a result of the ultrasonic examinations during the cycle run, it had been assumed no attack had occurred. It now appears that the tests did result in attack, but no sure nondestructive method is available for identifying such cracks. As an example, the Type 304 SS middle sheath must have had some attack through the entire wall to permit the steam to be exposed to the ID, yet no such crack was noted by visual or ultrasonic examination.

B. $FeCl_3$ Cycle Specification

Based on the results on the development summarized above, a $FeCl_3$ cycle was standardized to the specification given in Table VI.

TABLE VI

$FeCl_3$ CYCLE RUN OPERATING CONDITIONS

	Temperature °F			
Step No.	Inlet No. 1 Superheater	Outlet No. 2 Superheater	Outlet No. 3 Superheater	Days
1	546	650	630	1
2	546	560	550	2

Repetitive continuation of above.

0.5 ppm Cl^- as $FeCl_3$ in recirculating water.
Stresses on sheaths: as specified.
No heater in No. 3 superheat (air cooled).
20 ppm O_2 in steam.
2.5 ppm H_2 in steam.
1000 psi system pressure.

The chloride content added as $FeCl_3$ was increased to 0.5 ppm to bring the indicated failure time of the sensitized Type 304 SS to the desired rate of acceleration relative to the ESADE operation. The heater in the No. 3 superheater position was removed and a slight amount of internal air cooling used to take advantage of the knowledge gained from previous equipment failures (see following Section, page 31) and the published vapor pressure data on $FeCl_3$. (12)

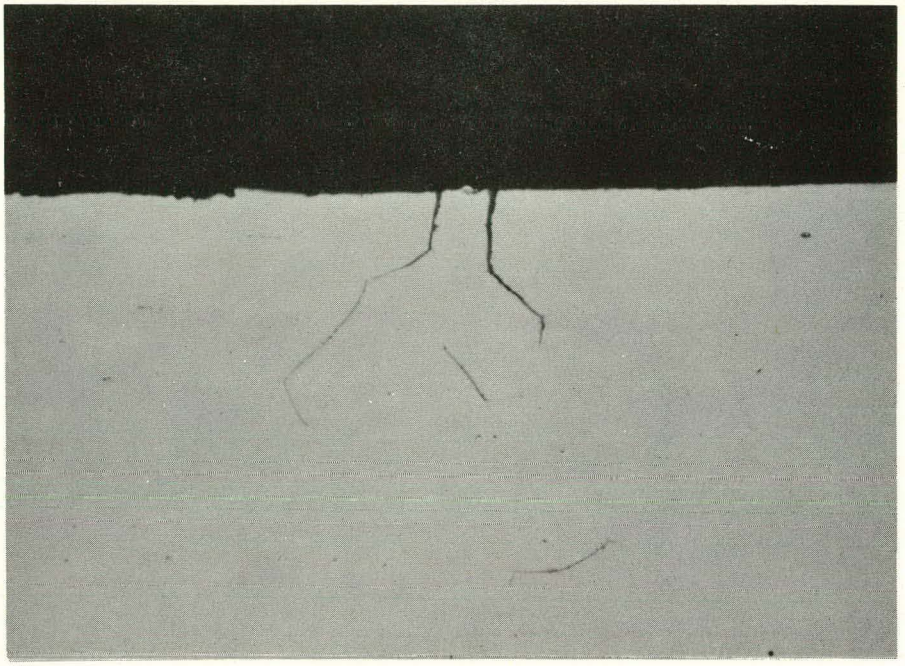

Figure 12. Type 316 SS $FeCl_3$ Development Cycle Run
Intergranular Attack Unetched 500X

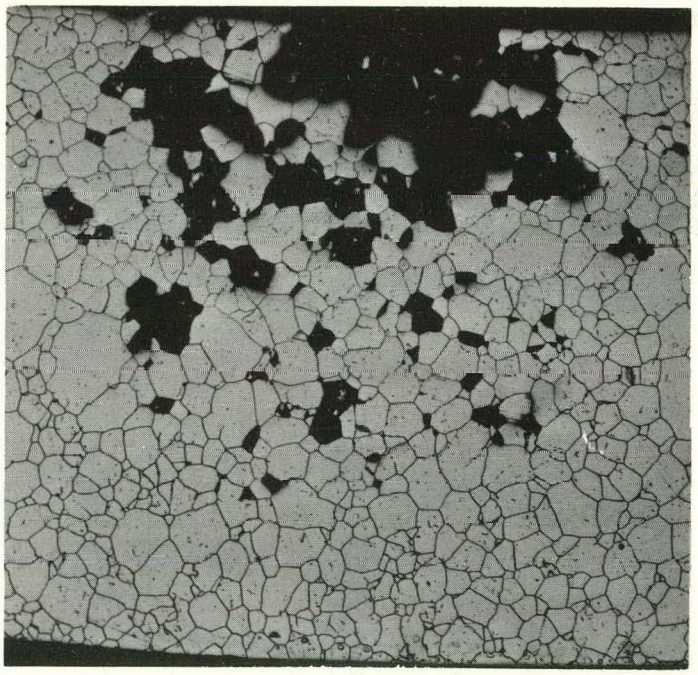

Figure 13. Type 304 SS $FeCl_3$ 100X
Development Cycle Run ID Attack
10% Oxalic Acid - Electrolytic
Etch, Grains Removed During
Metallographic Preparation

The effectiveness of the $FeCl_3$ cycle was demonstrated by exposing three new Type 304 SS sheaths (Code Y), that had been heat treated for 100 hours at 1100 F. The run was terminated after 44 hours of step two because of failure of the non-heated specimen in the No. 3 position. Examination up to 40X showed attack on all three sheaths. Metallographic examination indicated the attack to be intergranular. Figure 14a shows an attacked area as-polished and Figure 14b the same area after etching.

Figure 15 shows a portion of the area in Figure 14b at 750X. The attack is localized with the width being only slightly greater than the width of a grain boundary. The leading edges of the chemical attack are well indicated in the sensitized grain boundary structure shown in Figure 15.

A section of the cracked sheath was submitted for electron microscopic examination. The full details of the examination, as well as the techniques utilized are included as Appendix A. The microscopists summarized their findings: "The surface cracks under the plated-out layer are intergranular cracks filled with corrosion products. There was no evidence of deformation or primary mechanical cracking. The corrosion product fills the cracks to the very tip."

In the few electron microscopic examinations made of the ESH-1, Rod F failure, none of the type striations usually attributed to stress or stress cycling were found. (13) Although the contribution of stress and strain-cycling is an important variable to the failures, (13) the in-pile and out-of-pile results do validate a significant chemical attack contribution.

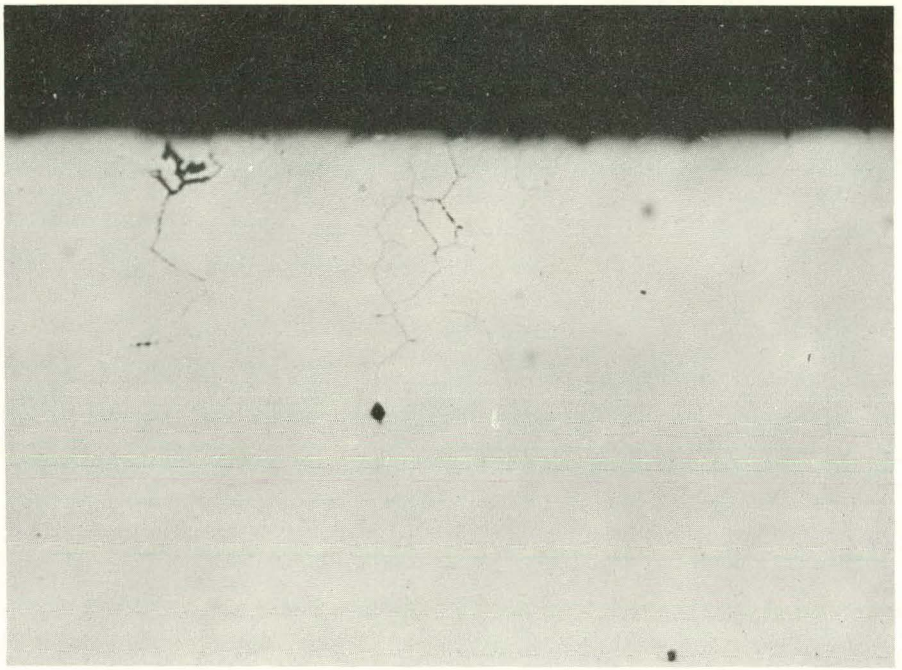

a. Unetched

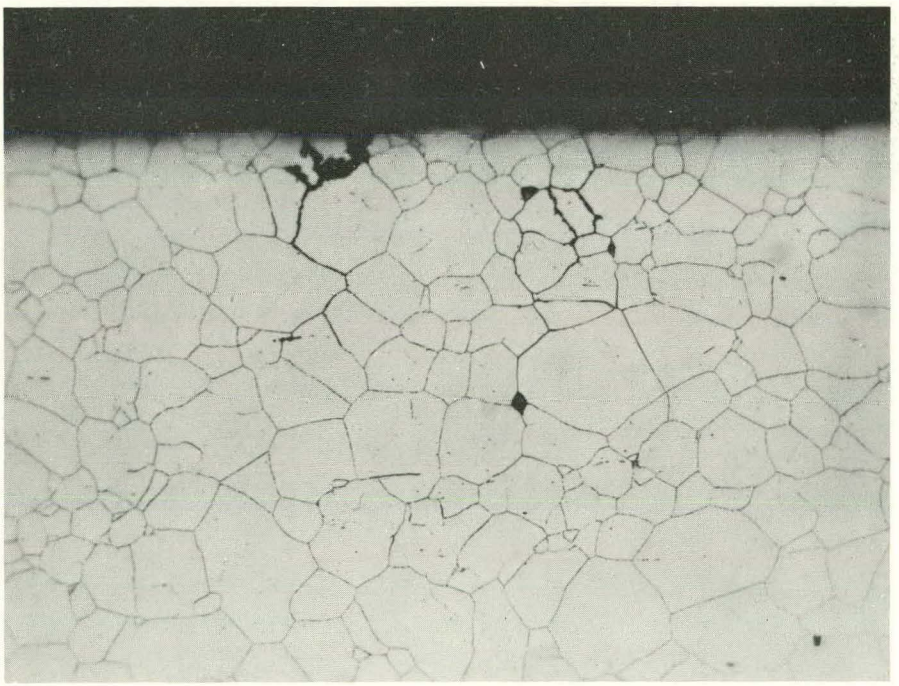

b. 10% Oxalic Acid Electrolytic Etch

Figure 14. Type 304 SS 44 Hours Exposure to $FeCl_3$ Cycle Run 250X

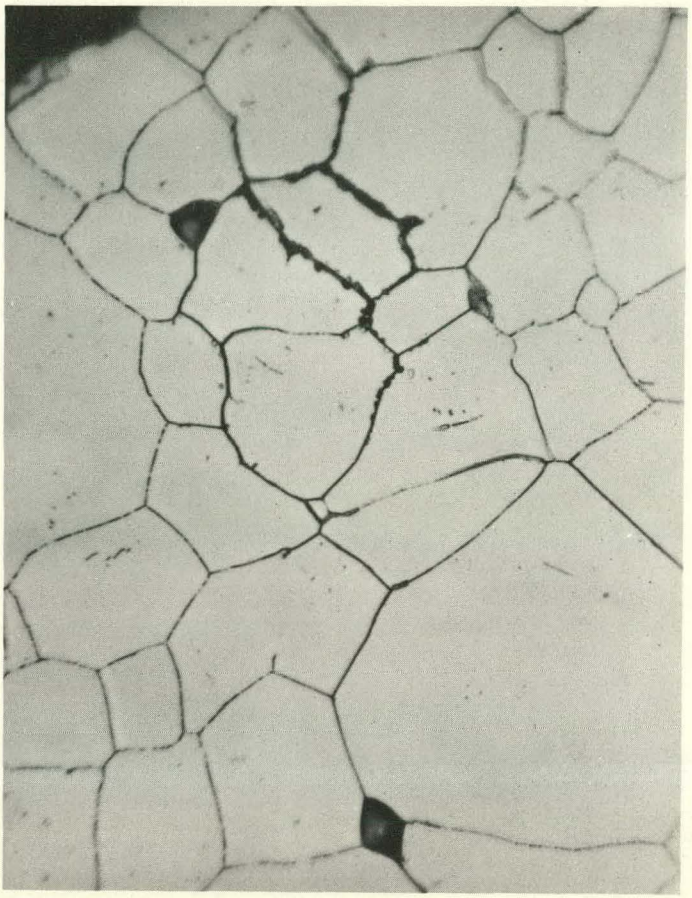

Figure 15. Type 304 SS 44 Hours Exposure to $FeCl_3$ Cycle Run
Enlargement of Figure 14b. 750X

EQUIPMENT FAILURES

During the development and carrying out of the NaCl-cycle runs, the CL-1 and CL-4 superheat facilities have been exposed to a myriad of conditions within the extremes of the test parameters involved. As such many pieces of equipment became useful test specimens in developing an understanding of type failures experienced in reactor systems over long periods of time. An attempt is made to include in this section those equipment experiences that are of interest and have some bearing on materials performance in SHR systems.

A. Desuperheating System

The 1050 F, 1000 psi superheated steam from the superheat coupon section of both the CL-1 and the CL-4 facilities is introduced into the desuperheater-steam generator (see Figure 1), commonly referred to as the desuperheater section. Here the superheated steam passes through 21 feet of 0.50-inch OD × 0.035-inch wall annealed Type 316 SS tubing transferring heat to the steam-water mixture flowing over the outside of the tube. This tubing is coiled within a section of 4-inch schedule-80 pipe which forms the outer pressure vessel as shown in Figure 16. In this manner the desuperheater section generates 50 percent additional steam in the 545 F steam-water mixture to increase the steam flow through the superheat portion of each facility.

The superheat remaining in the steam after passing through the desuperheater-steam generator is dumped to the condensate returning to the recirculation pump by means of a feedwater heater. The superheated steam passes through 21 feet of 0.50-inch OD × 0.042-inch wall annealed Type 304 SS tubing transferring heat to the feedwater flowing over the outside of the tube. This tubing is coiled within 18 feet of 0.875-inch OD × 0.065-inch wall annealed Type 304 SS tubing which carries the feedwater. The actual heat exchange accomplished in practice was minimal with the superheated steam entering at about 546 F (900 psig pressure) and the feedwater entering the outer coil at about 530 F (1000 psig).

Complete details of the equipment were included in a previous publication.[9]

1. CL-1 Desuperheater Coil

The Type 316 SS desuperheater coil of the CL-1 facility failed after about 13,600 hours of operation. The facility had been operated for general corrosion testing about 10,000 hours with no added chlorides and for the NaCl cycle for the remaining 3600 hours utilizing 1.5 ppm chlorides in the recirculating water. The coil had failed near the outlet end where the superheated steam decreased to a temperature no higher than 650 F. Other cracks were noted only in the vicinity of the failure.

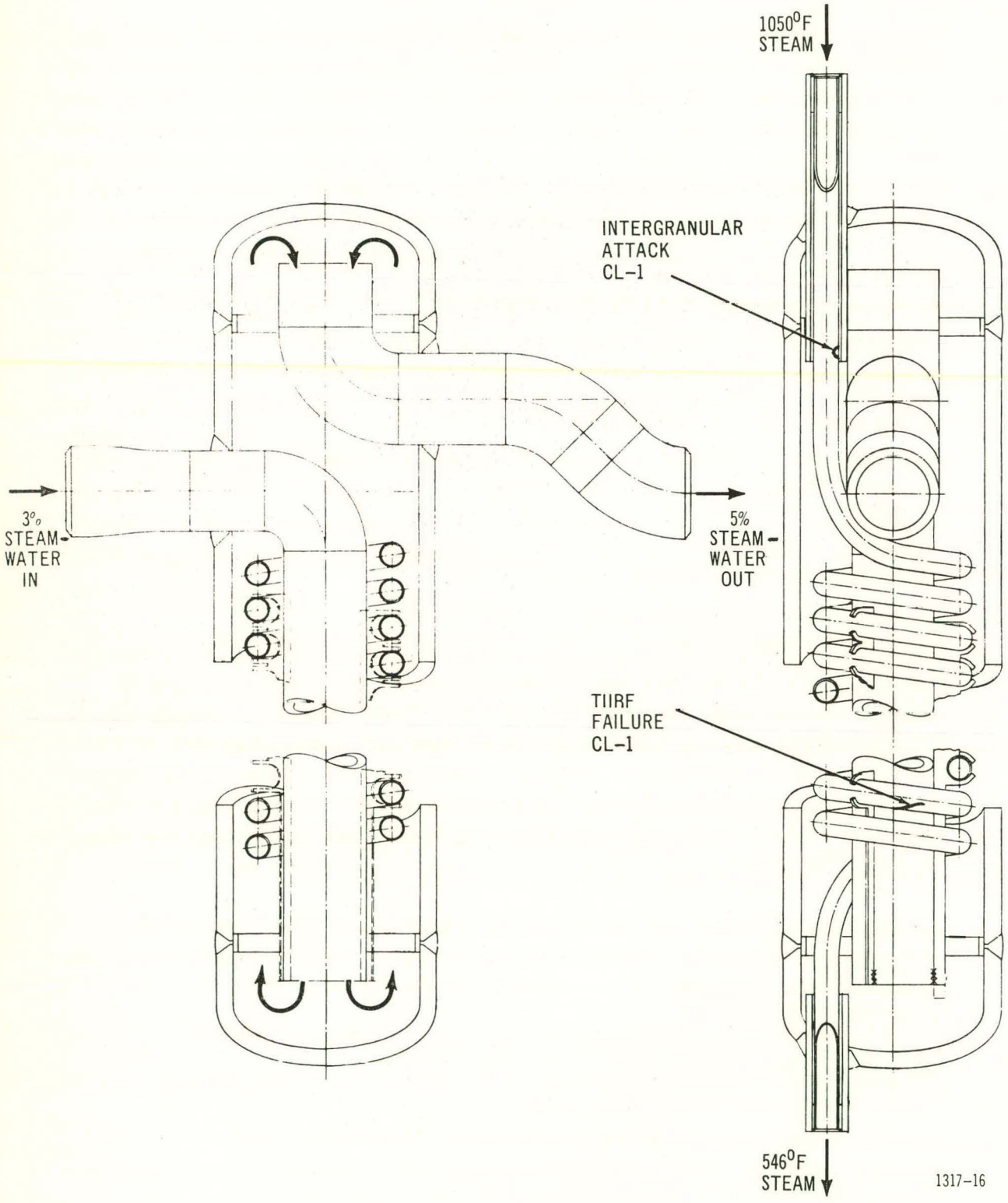

Figure 16. Desuperheater Section of the Superheat Facilities

The inside surface of the sectioned coil was grey in color at the hot end with a light brown to orange color at the outlet end. Metallurgical evaluation indicated the failure to be transgranular attack with small transgranular and intergranular cracks leading from the main attack, see Figure 17. The inlet of the coil, which had been exposed to 1050 F steam for at least 12,000 hours, was found to be completely sensitized and subjected to intergranular attack as shown in Figure 18. The intergranular attack was found on the straight portion of the coil. The presence of significant stress in this area probably would have resulted in a more directionally oriented attack than seen in Figure 18.

A considerable stress was put in the coil during forming. The source of the chemicals that might cause the apparent attack was not as obvious. Although 1.5 ppm of chloride as NaCl was maintained in the boiler water, no NaCl has been noted on the deposits found on the superheater sheaths.(3) Straub(14) had demonstrated that a steam containing mechanically entrained boiler water would dissolve sodium chloride as the steam was superheated. The sodium chloride would then precipitate out as the temperature and pressure of the steam were reduced. Other salts such as the chlorides of iron and copper present in the system might similarly be transported through the system and play a part in such attack as noted in the desuperheater coil. Any deposits would have been wetted during startup and shutdown periods.

2. CL-4 Desuperheater Coil

The Type 316 SS CL-4 desuperheater coil failed after ~2900 hours of NaCl-cycle exposure of which about 700 hours were with 1050 F inlet superheated steam. The through failures were found at both the hot and cold ends of the coil as well as fine visible cracks all along the coil. A white deposit was visible in some of the cracks. After sectioning, many cracks were visible on the inside of the coil in various positions along the surface. At the cold end, a thin white deposit completely coated the inner surface of the coil.

Metallographic sections taken through the large open cracks at both the hot and cold ends revealed the cracks to be transgranular with many smaller transgranular cracks in the sections, see Figure 19, for example. No indication of sensitization was noted at the hot end of the coil.

The attack at the lower temperature end of the CL-4 coil was more obviously a typical chloride stress corrosion cracking because of the apparent depositing of sodium chloride. The substantial buildup of salts can be understood in this case, since the amount of moisture carryover with the steam is much greater in the CL-4 superheat facility than in the CL-1 facility as noted previously (page 13).

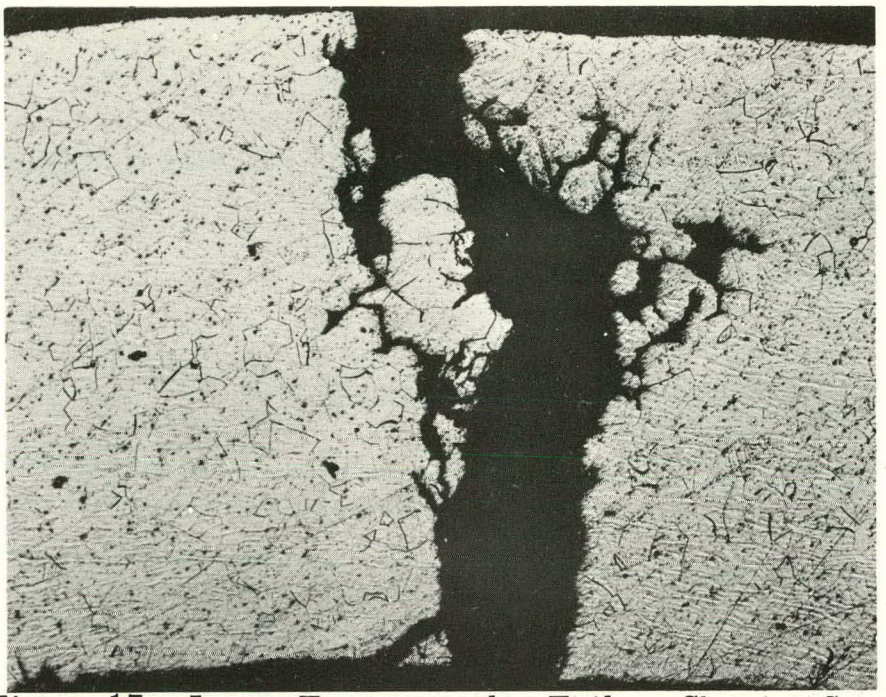

Figure 17. Large Transgranular Failure Showing Small Transgranular Cracks and Some Intergranular Attack Leading From It.
Vilella's Etch 100X

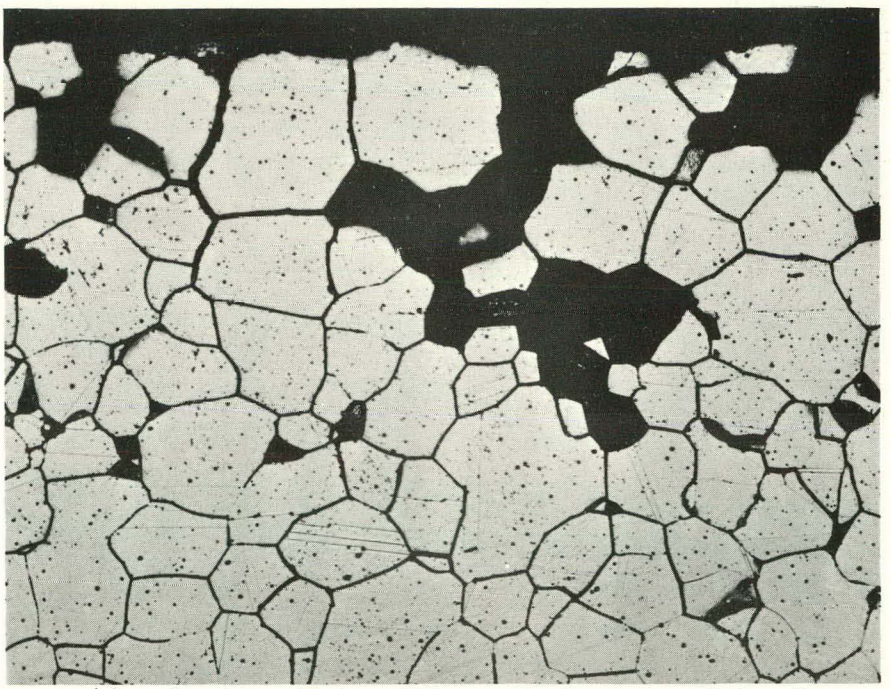

Figure 18. Section Taken Through the Inlet Tube Showing Sensitization, Intergranular Attack, and Missing Grains. Vilella's Etch 250X

Figure 19. Section Through Hot-Leg of the CL-4 Desuperheater Coil Showing Transgranular Cracks, 60% Nitric Acid Electrolytic Etch 250X

The lack of sensitization of the hot end of the coil can be accounted for only by the probability that the metal temperature was somewhat below the 1050 F superheated steam temperature and 700 hours was not sufficient time to produce detectable sensitization.

3. CL-4 Feedwater Heater

The Type 304 SS feedwater heater had been in the CL-4 facility for the same 2900 hours of NaCl-cycle runs as the previously described desuperheater coil. A failure was found in the inner coil with numerous fine cracks starting at the superheated steam inlet and continuing for two-thirds of the length of the coil. The through crack contained a white deposit. Areas with small stains on the surface were sectioned and found to contain small cracks. Again the cracks were found to be transgranular.

B. Superheat Piping

The CL-1 and CL-4 superheat facilities are well insulated so that all piping from the outlet at the exit superheater to the inlet of the desuperheater is exposed to superheated steam essentially at 1050 F.

1. Superheat Coupon Holder Cover Plate

A cover plate utilized with a superheat coupon holder in CL-4 was found to be cracked. The holder had been in the superheat coupon section during the NaCl-cycle runs for a total of 1728 hours of which 466 hours were at 1050 F. A cross section of a mounted cover plate is shown in Figure 20. When the coupon holder is in place in the superheat

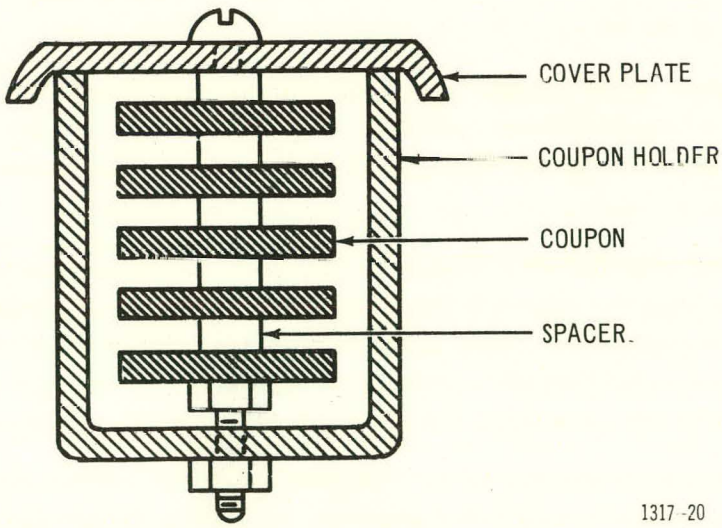

Figure 20. Schematic of Loaded Coupon Holder

coupon section, the 1050 F steam flows through the holder at about a 20 fps velocity contacting the inside surface of the cover plate. The coupon holder is so designed to permit an insulating layer of essentially static 1050 F steam between the coupon holder (outside surface of the cover plate) and the coupon section pressure piping.

The composition of the cover plate was Type 304 stainless steel. It had several visible cracks leading from the screw holes. Further examination with a stereo microscope at magnifications up to 40X revealed additional cracks. Due to the overtightening of the bolts, the cover plate had become bent with the inside surface in tension and the outer surface in compression.

Metallographic examination revealed that the cover plate had a sensitized structure which was intergranularly attacked, as shown in Figures 21 and 22. The cracks initiated at the tensile edge as shown in Figure 21. However, intergranular attack was noted at both the tensile and compressive surfaces as shown in Figure 23.

The cover plate at 1050 F for 466 hours resulted in complete sensitization of the Type 304 SS structure. Although the intergranular cracks were apparently caused by a chemical attack, the tensile stresses on the inside surface opened up the cracks and helped speed the intergranular attack perpendicular to the stress. The cracks on the compressive surface indicate that tensile stresses are not a prerequisite to the type attack noted. Moisture was available for the chemical attack during the shutdown and startup periods of the facility.

2. Superheated Steam Sampler

A steam sampler located at the outlet of the exit superheater position started to leak adjacent to the ferrule connection. The sampler was utilized during the NaCl-cycle runs for a total of about 2000 hours of which 1050 F superheated steam was generated one-quarter of the time.

The composition of the sampler was Type 304 stainless steel. The metal temperature at the point of failure reached near 1050 F only at the time of sampling. Figure 24 is a schematic showing the positioning of the sampler and ferrule through the pipe wall and the areas of failure.

Metallographic examination revealed the failure to be transgranular with other transgranular cracks in the region of the ferrule and in the ferrule itself. Figure 25 shows a region of transgranular cracks in the sampler section adjacent to the ferrule. Further examination revealed that the section of the sampler tube that was in the 1050 F steam path was completely sensitized and intergranularly attacked as shown in Figure 26.

The intergranular attack was tied to chemical action not necessarily in conjunction with stress with indications distributed generally on both the ID and OD of the straight piece of sampler tubing. The transgranular failures in the region of the ferrule were more a typical stress corrosion attack in the presence of the high stresses resulting from the ferrule application.

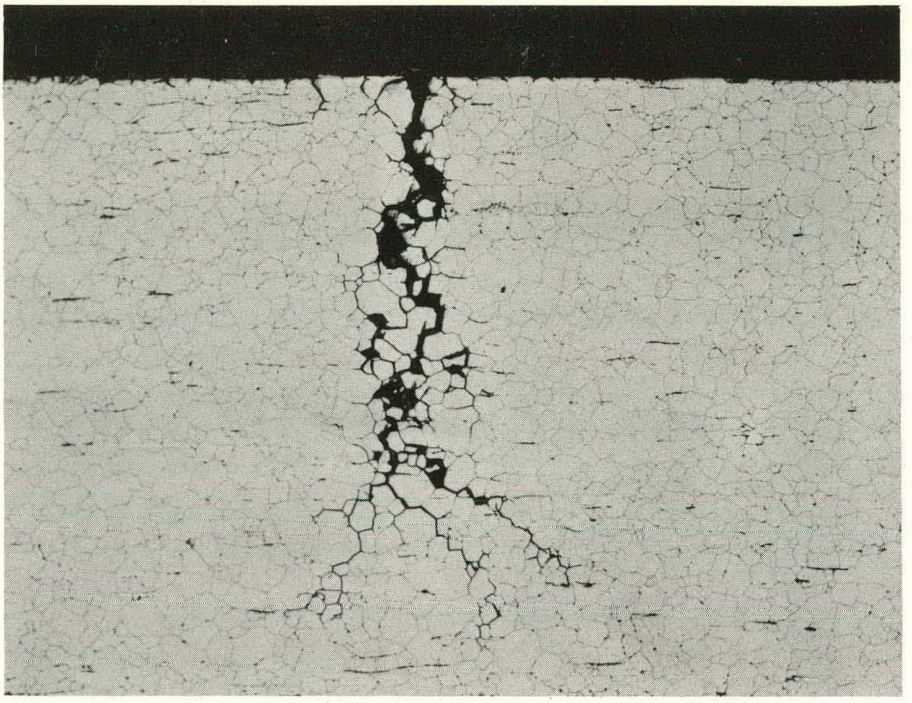

Figure 21. Section Through Cover Plate Exposed at 1050 F Showing Sensitized Structure With Intergranular Crack. 10% Oxalic Acid - Electrolytic Etch 100X

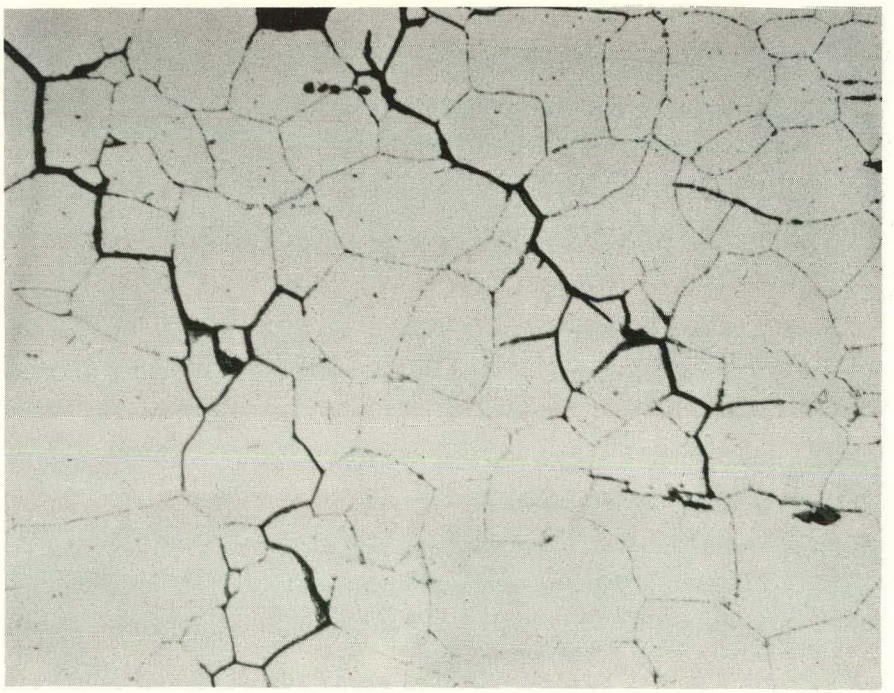

Figure 22. Enlarged Section of Cover Plate Shown in Figure 21. 10% Oxalic Acid - Electrolytic Etch 500X

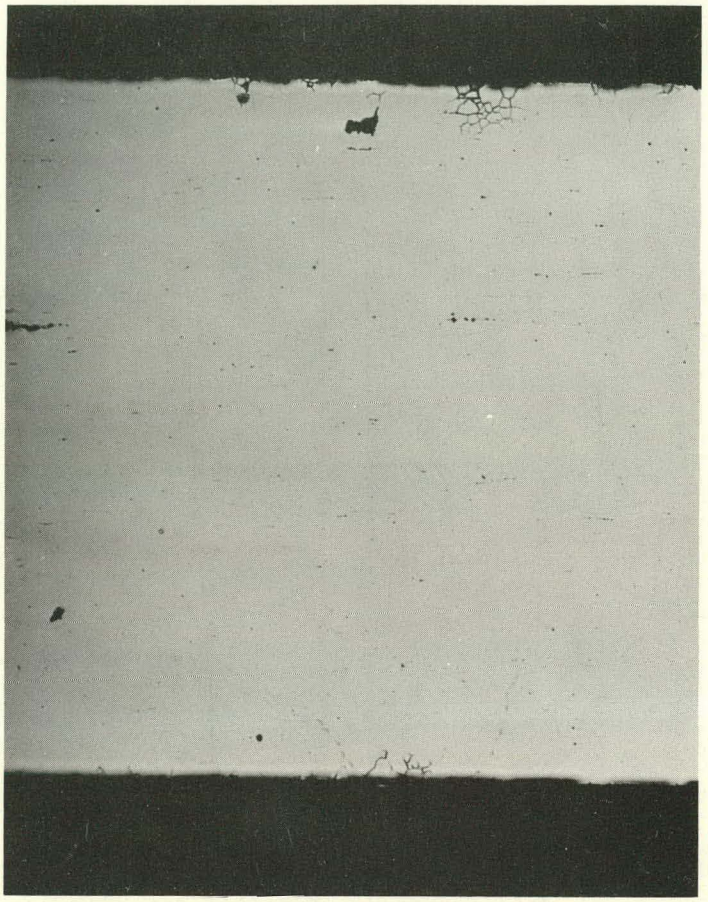

Figure 23. Intergranular Attack of Cover Plate Shown at Both the Tensile and Compressive Edges Unetched 75X

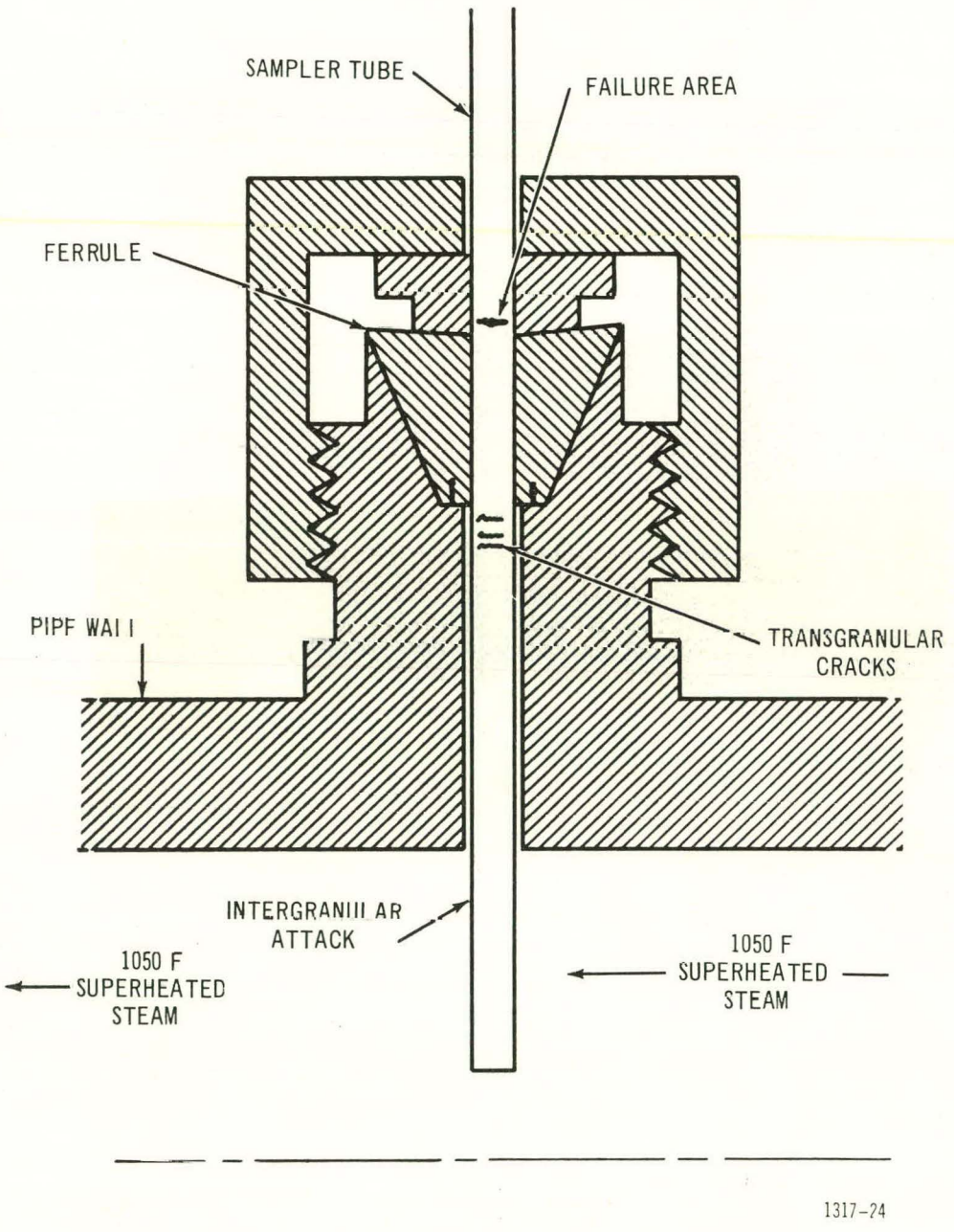

Figure 24. Sampler Location Schematic Illustrating the Failure Areas

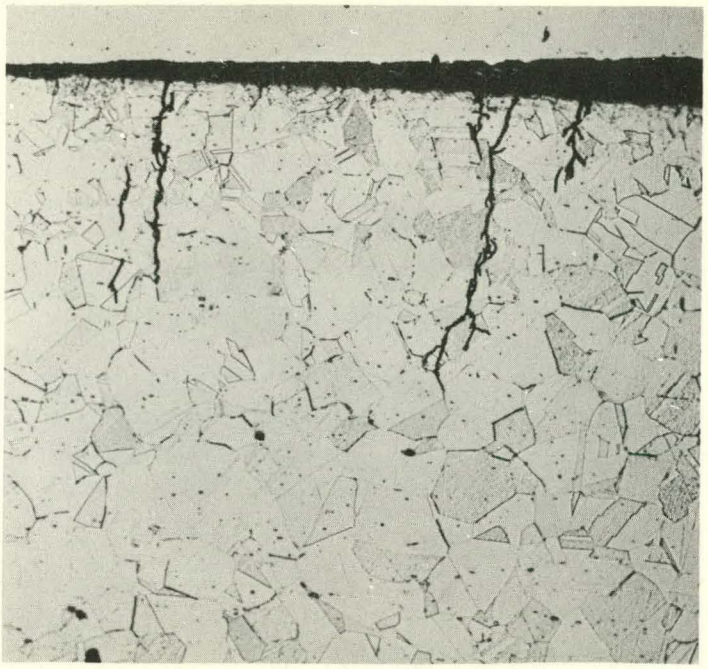

Figure 25. Section Through Superheat Sampler Adjacent to Ferrule Showing Transgranular Cracking 10% Oxalic Acid Electrolytic Etch 250X

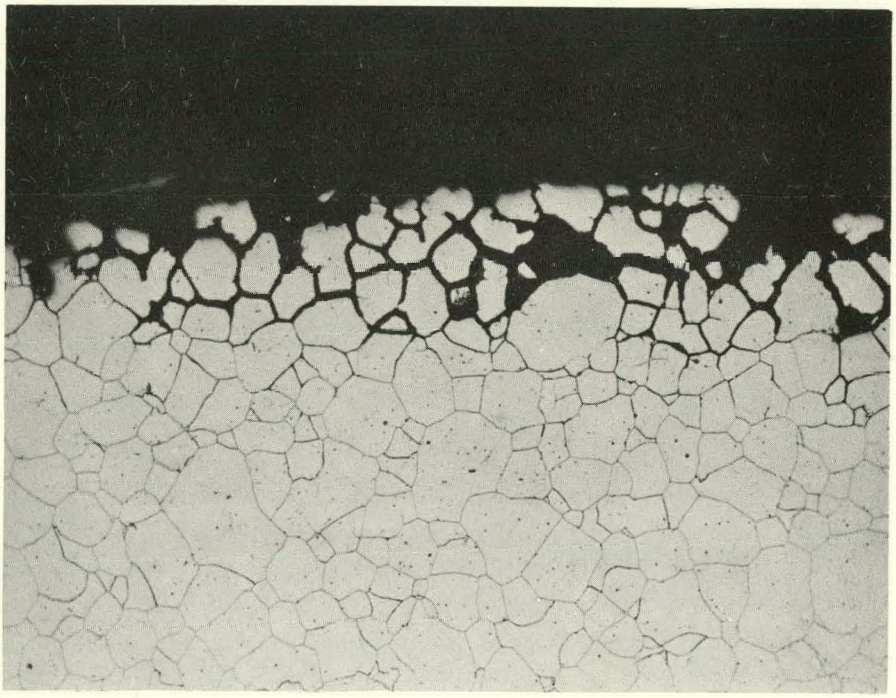

Figure 26. Section Through Superheat Sampler Tube Protruding in 1050 F Steam Path, Showing Intergranular Attack, 10% Oxalic Acid Electrolytic Etch 250X

DISCUSSION

The localized attack studies and equipment failures described previously have added significantly to our understanding of the type of reactions involved in the SADE and ESADE fuel cladding failures. Although the actual chemical involved in the intergranular attack has not been established, it has been possible to empirically simulate the type failure out-of-pile.

The interplay of the chemical attack and stress cannot be overemphasized. Chemical attack will occur essentially independent of stress, as occurred in the straight portions of the CL-1 desuperheater coil and sampler tube, but the attack is generally distributed (Figures 18 and 26) and slow to decrease the integrity of the tubing in cross section. It is hypothesized that the application of stress will speed up the intergranular attack perpendicular to the stress by opening the previously attacked area to permit more rapid refreshment of the attacking chemical and/or constantly subjecting unexposed grain boundaries to the corrosive media. As the cross section of resistance to the stress is gradually decreased by such chemical attack, the locally applied stress may increase to the point where the final failure becomes purely mechanical.

The heat treating of the 300 series stainless steels in the temperature range of sensitization has been indicated as a prerequisite to the intergranular attack. Although it is realized that such intergranular attack has been experienced in Types 304 and 347 SS in the absence of such sensitization, [15,16] the operation of a SHR system essentially infers the operation of at least part of the fuel cladding in the sensitizing temperature range. This was recently well emphasized in electron microscope fractography studies of the ESH-1, Rod F failure. [13] The clad apparently had been subjected to a myriad of temperatures and combination of temperatures that will precipitate the many types of carbides found in the failed Type 304 SS. The preferential deposition of such carbides in the grain boundaries has made these austenitic materials more susceptible to intergranular chemical attack in the presence of certain chemicals. Others have shown that the specific form that the carbide exists in the grain boundaries has a definite influence on susceptibility to intergranular attack. [17] This consideration is important in trying to duplicate in-pile failures with out-of-pile tests, since the most susceptible form (and temperature for obtaining same) for each material is not known.

The form of the chemical also is critical. For example, chlorides per se do not account for the failures experienced. Sensitized Type 304 SS tested in boiling 42 percent $MgCl_2$ has resulted in transgranular cracking and then only in the presence of very high stresses. The use of such a chloride results in the typical chloride stress corrosion cracking and is not representative of the failure mechanism of interest in the present study.

The oxidizing chloride, $FeCl_3$, has successfully produced the type chemical attack experienced in the in-pile failures. It is not known that $FeCl_3$ is the specific chemical or only chemical causing the attack either in-pile or out-of-pile. The knowledge that the ferric ion and chloride ion are

present in a reactor system and the fact that the chemical attack will occur makes the use of $FeCl_3$ an excellent means for comparing the susceptibility of various materials to such attack.

It is important to note that the $FeCl_3$ cycle developed does not utilize operation at high superheat temperatures but that the chemical attack occurs at or near the boiling operation temperatures. This concept assumes that the contribution of high superheat temperatures is primarily to sensitize the material and in the case of in-reactor operation to apply the stresses that help accelerate the chemical attack at boiling temperatures as described above.

The results of the 300 series stainless steels tested within the scope of this report have supported the attack mechanism hypotheses. The commercial Types 304, 347, and 316 SS have all tested as susceptible. The use of vacuum melted Type 304 SS with high or low carbon content has not shown a significant improvement in susceptibility to intergranular attack, although it has been demonstrated that such materials are more resistant to typical chloride stress corrosion as represented in $MgCl_2$.[7,8,11]

The presence of the molybdenum in Type 316 SS probably would minimize any beneficial effect that could be hoped for by use of low carbon.[18]

The higher nickel and/or chromium present in Type 310 SS has shown up as beneficial within the limits of the tests performed to-date. The contribution of the vacuum melting (low nitrogen) in the relative resistance to attack has not yet been factored into the test program.

The present work has shown a limitation of the ultrasonic testing now in use for indicating the degree of cracking present though it is very effective in finding through cracks of fuel element cladding. It is hoped that the development of suitable nondestructive testing standards will improve the ability to determine the depth of intergranular attack by such means.

ACKNOWLEDGMENTS

The authors gratefully acknowledge the assistance of the Corrosion Engineering Group under the direction of M. Siegler for the operation of the CL-1 and CL-4 superheat facilities; D. F. MacMillan, who performed most of the metallography; T. G. Lambert, who carried out the ultrasonic testing; R. F. Kirby, who procured most of the special test materials; Miss U. E. Wolff and W. C. Cowden for their electron microscopic examinations; and the many other members of the Vallecitos Laboratory who contributed their efforts and counseling in making the work possible.

REFERENCES

1. Spalaris, C. N., Boyle, R. F., Evans, T. F., and Esch, E. L., GEAP-3796, "Design, Fabrication, and Irradiation of Superheat Fuel Element SH-4B in VBWR", September 1, 1961.

2. Spalaris, C. N., "Fuel Element Experiments in SADE-VBWR Nuclear Superheat Loop", GEAP-4240, May 1963.

3. Gaul, G. G., Pearl, W. L., and Siegler, M., GEAP-4025, "Stress Corrosion of Type 304 Stainless Steel in Simulated Superheat Reactor Environments", February 26, 1962.

4. Spalaris, C. N., Comprelli, F. A., Douglass, D. L., and Reynolds, M. B., GEAP-3875, "Materials for Nuclear Superheat Applications", A Literature Survey, January 5, 1962.

5. Pearl, W. L. and Gaul, G. G., GEAP-4165A, "General and Stress Corrosion of High Nickel Alloys in Simulated Superheat Reactor Enviroment", March 1963.

6. COO-266, "Proceedings of the Nuclear Superheat Meeting No. 7", September 12-14, 1962, Sioux Falls, South Dakota, October 30, 1962.

7. Lang, F. S., "Effects of Trace Elements on Stress-Corrosion Cracking of Austenitic Stainless Steels in Chloride Solutions", Corrosion 18:378t-382t (1962).

8. Uhlig, H. H. and White, R. A., "Some Metallurgical Factors Affecting Stress Corrosion Cracking of Austenitic Stainless Steels", Trans ASM, 52:830, (1960).

9. Fitzsimmons, M. D., Pearl, W. L., and Siegler, M., GEAP-3778, "A Simulated Superheat Reactor Corrosion Facility", August 14, 1961.

10. Gaul, G. G. and Pearl, W. L., GEAP-3779, "Corrosion of Type 304 Stainless Steel in Simulated Superheat Reactor Environment", October 16, 1961.

11. GEAP-4153, "Nuclear Superheat Project Fourteenth Quarterly Report, October-December, 1962".

12. International Nickel Company, "Resistance of Nickel, Monel, and Other High Nickel Alloys to Corrosion by Hydrochloric Acid, Hydrogen Chloride, and Chlorine", Technical Bulletin T-29, December, 1945.

13. GEAP-4243, "Nuclear Superheat Project Fifteenth Quarterly Report, January - April, 1963".

14. Straub, F. G., "Steam Turbine Blade Deposits", Eng. Exp. Station Bulletin 364, University of Illinois, Urbana, Illinois, June 1, 1946.

15. Wanklyn, J. N. and Jones, D., "The Corrosion of Austenitic Stainless Steels under Heat Transfer in High Temperature Water", J. of Nuclear Materials 2:154-173, (1959).

16. Holliday, R. L., GEAP-4155, "High Power Density Development Project Eleventh Quarterly Progress Report, October-December 1962".

17. Stickler, R. and Vinckier, A., "Morphology of Grain Boundary Carbides and Its Influence on Intergranular Corrosion of 304 Stainless Steel", Trans. ASM, 54, 362 (1961).

18. Heger, J. J. and Hamilton, J. L., "Effect of Minor Constituents on the Intergranular Corrosion of Austenitic Stainless Steels", Corrosion, 11:22-6 (1955).

GENERAL ELECTRIC COMPANY
VALLECITOS ATOMIC LABORATORY
Pleasanton, California

MEMO REPORT

ELECTRON MICROSCOPIC EXAMINATION OF STAINLESS STEEL TUBING FAILED IN SUPERHEAT LOOP

by

U. E. Wolff
W. C. Cowden

Metallurgy
Vallecitos Atomic Laboratory

June 17, 1963

APPENDIX A

A. INTRODUCTION

The following information concerning experimental conditions was obtained from G. G. Gaul:

As part of the Superheat Program, U. S. Atomic Energy Commission Contract No. AT(04-3)-189, Project Agreement No. 13, Type 304 stainless steel tubing, 0.564 inch OD, 0.500 inch ID, had been pre-sensitized 100 hours at 1100 F prior to exposure in the superheat loop. During loop exposure in the temperature range of 550 to 600 F the tubing was under a longitudinal stress of 25,000 psi. No cycling was involved. The water for the superheat steam contained 1/2 ppm chloride ions added as iron chloride. The tubing failed in less than three days.

Visual inspection of the tubing revealed streaks of reddish-brown surface deposits concentrated in certain areas. Underneath these deposits numerous transverse surface cracks were observed. No cracks were seen in areas without the deposit.

A sample of the tubing containing the deposit and cracks was received for investigation of the cracking mechanism.

B. EXPERIMENTAL PROCEDURES

Optical and electron microscopy were used for examining the failed tubing. Three methods were employed, each of which will be discussed separately.

1. Microscopy of metallographic section of tubing wall containing part-through cracks.
2. Fractographic examination of low temperature fracture by extraction replication.
3. Selected area diffraction of corrosion product.

1. Metallographic Section

A section through the tubing wall, parallel to the tube axis and containing visible cracks was prepared for metallography. After optical microscopy the same surface was replicated for electron microscopy using a two-stage plastic-carbon replica.

A softened piece of cellulose acetate was pressed against the surface to be examined, allowed to dry, and stripped. Chromium was evaporated onto the replica at an angle of 35 degrees to the surface, followed by a thin carbon film at normal incidence. To prevent break-up, molten wax was dropped onto the carbon side. The cellulose acetate was dissolved in acetone, and then the wax was dissolved in xylene. The resulting Cr-shadowed carbon replica of the desired surface was then washed, dried, and examined in the electron microscope.

2. Fractography

A piece of the tubing containing the plated out corrosion product and part-through cracks was fractured at liquid nitrogen temperature under impact loading. This was done for the dual purpose of exposing an original crack surface and of checking for sensitization. An extraction replica technique was then employed to extract non-metallic inclusions and to obtain information on the fracture topography.

A 50 Å thick carbon film was evaporated directly onto the fracture surface. The fractured steel was then immersed in a 10 percent bromine-alcohol solution which dissolves the matrix but leaves carbides and other nonmetallic inclusions unattacked. When the carbon film floats free of the fracture surface, it contains, embedded in it, the insoluble inclusions that were exposed on the fracture surface. The resulting replica was washed, dried and examined in the microscope. Electron micrographs of the fracture were made as stereo-pairs to aid in interpreting the fracture topography.

3. Diffraction of Corrosion Product

The extraction replica technique described above was used to extract the corrosion product from the tube surface as well as from the small dark areas of the fracture surface (see Figure A-4). These replicas were examined by electron microscopy and electron diffraction.

C. RESULTS

1. Optical and Electron Microscopic Observations on Metallographic Section

Figure A-1 shows the whole wall thickness of the tubing. The outer surface contains numerous short cracks which are all intergranular. Figure A-2 shows one of them in higher magnification. Slight bending of the sample has opened up this particular crack.

An electron micrograph of one of the crack tips is shown in Figure A-3. The crack apparently is filled with corrosion product to its very tip. There is no evidence of deformation, slip, or mechanical cracking ahead of the corrosion crack. This finding is similar to corrosion cracks found in other fuel cladding failures and argues strongly for a primary corrosion cause of the failure. This does not mean to imply, though, that the applied stress might not have enhanced the corrosion.

2. Fractography

Since the tubing was intentionally sensitized, it was no surprise that the low temperature fracture was intergranular and brittle (Figure A-4). The electron micrographs, Figures A-5 and A-6, show clearly the intergranular nature of the low temperature impact fracture, especially in three dimensional viewing of stereo-pairs. The grain boundaries are covered with uniformly shaped chromium carbide precipitates which have either been extracted (black

OD ID

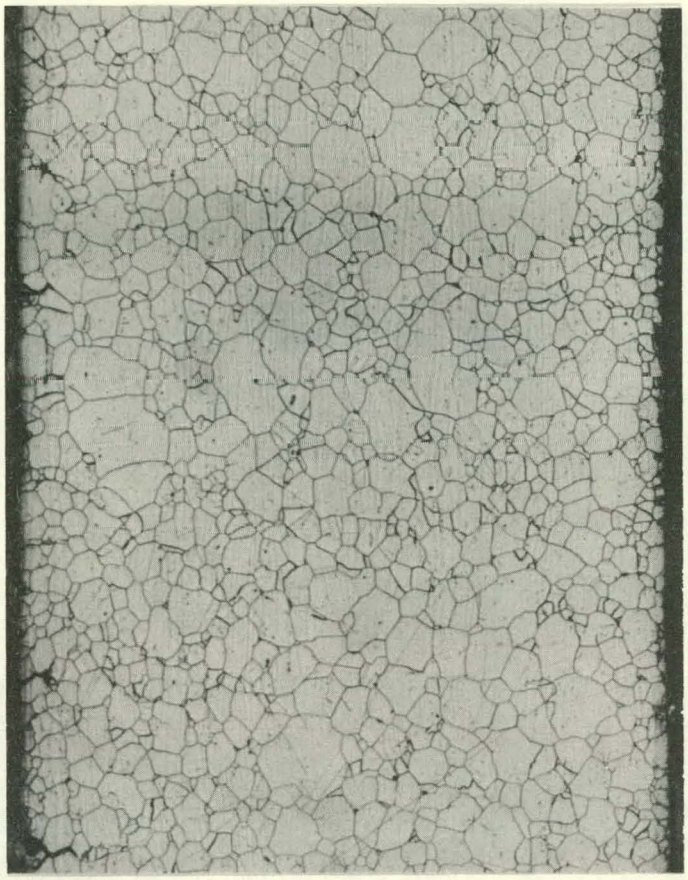

Figure A-1 100X

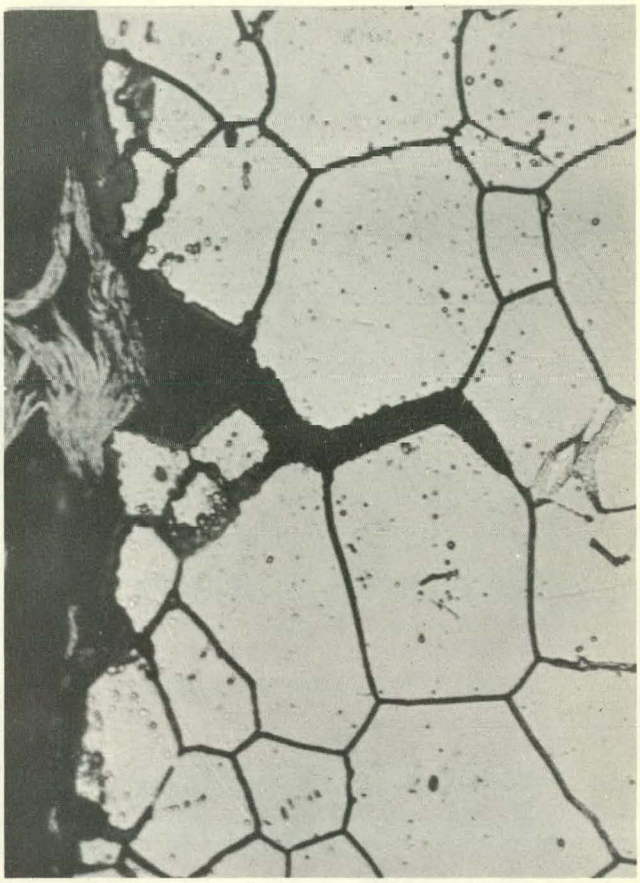

Figure A-2

Intercrystalline Cracks at OD of Tubing

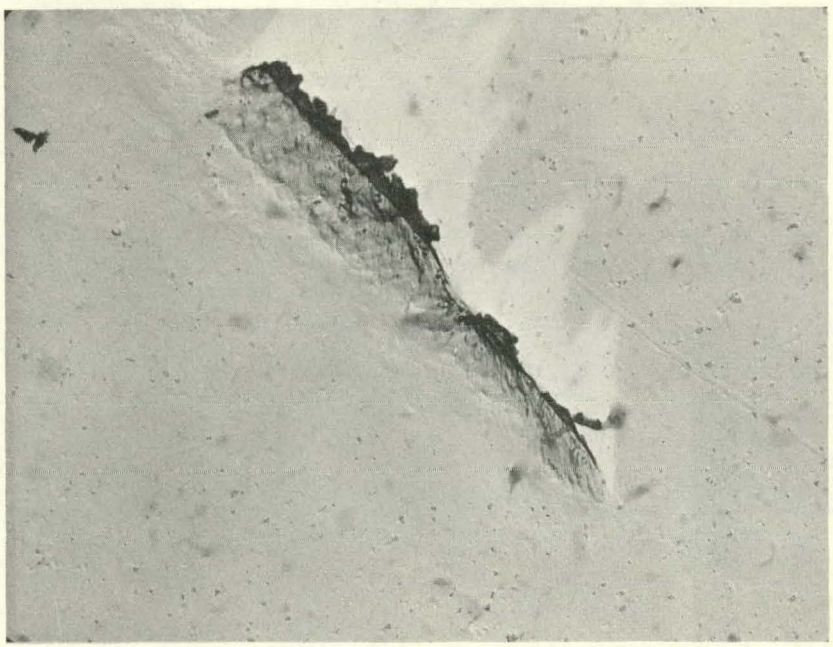

Figure A-3 18,000 X

Plastic replicating material stands above replica surface, indicating a narrow crack between corrosion product and side of intergranular crack. The white area is the shadow cast by that plastic.

Electron Micrograph of Crack Tip Replica

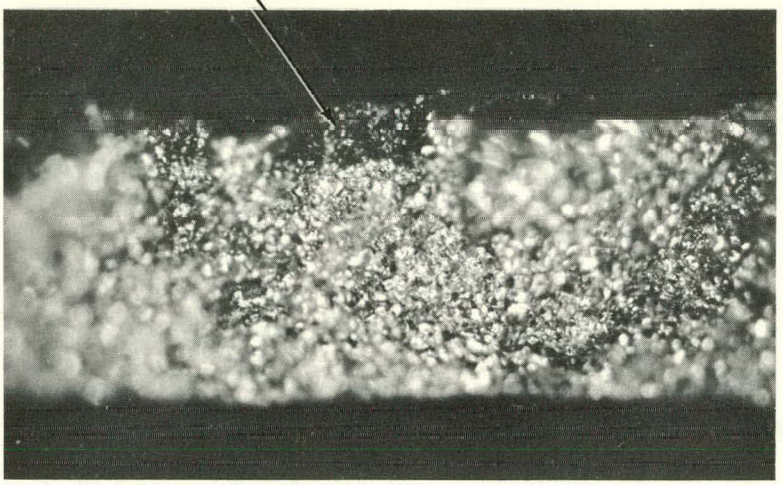

Figure A-4 50X

Low Temperature Impact Fracture Surface

Figure A-5 6000X

Figure A-6 6000X

Electron Micrographs of Extraction Replica of Low Temperature Impact Fracture. Dark Carbide Precipitates on Grain Boundaries.

triangles, etc. in Figures A-5 and A-6) or have left depressions which appear in the replica as uniformly spaced outlines of the same shape as the extracted carbides.

At the outer tubing surface there are several dark spots (see arrow in Figure A-4) which apparently are the incipient cracks present before the impact fracture. Extraction replicas from these spots revealed a rather thick (for electrons) continuous film of corrosion products lying on top of the other features just described. Figure A-7 shows the edge of this film. The film was similar in morphology (but not in diffraction pattern) to the films observed in other fuel cladding failures.

A similarly thick corrosion film extracted from the tube surface is shown in Figure A-8. Stereo viewing reveals that the dark areas are actually films standing vertical and obviously pulled out of grain boundaries.

3. Diffraction

The electron diffraction pattern produced by the corrosion film of Figure A-8 is shown in Figure A-9. The same pattern was obtained from the film in Figure A-7. Indexing and analysis of the pattern revealed that the extracted product has fcc crystal structure with a lattice parameter of approximately 8.4 Å. (See Table A-I). The ASTM card file lists several spinel type oxides of Fe, Cr, Ni, Mn, etc. in varying combinations which have similar lattice constants and all of which would be possible in the superheat steam environment. Unambiguous identification, therefore, is not possible by electron diffraction alone.

X-ray fluorescent analysis or some other means of chemical analysis might aid in positive identification.

D. SUMMARY

The surface cracks under the plated-out layer are intergranular cracks filled with corrosion product. There is no evidence of deformation or primary mechanical cracking. The corrosion product fills the cracks to the very tip.

Electron diffraction patterns of the corrosion product revealed a fcc structure with a lattice constant of approximately 8.4 Å. A number of Fe, Cr, Ni, Mn or similar spinels in varying proportions could account for this pattern.

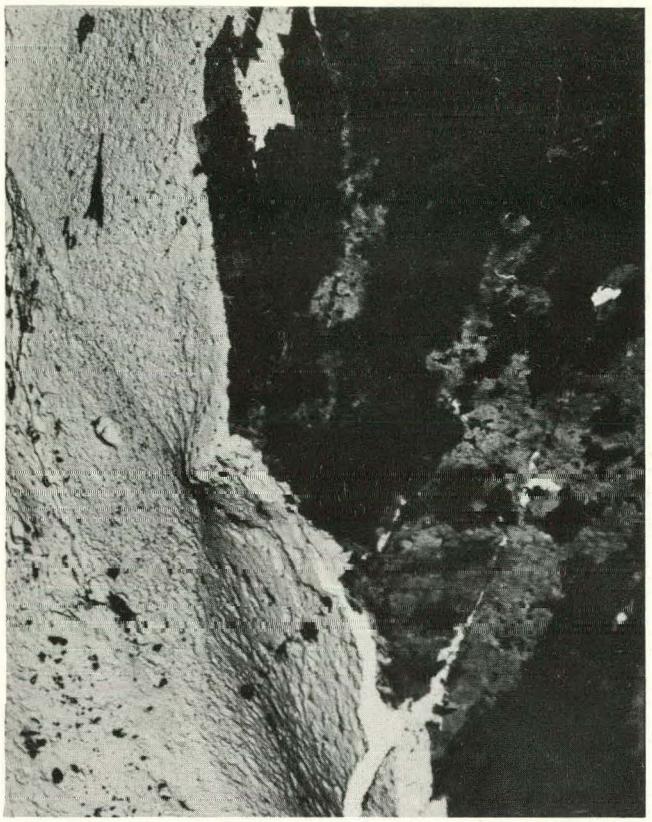

Figure A-7 6000X

Fracture Extraction Replica
With Corrosion Product On
Dark Spot Of Fracture Surface

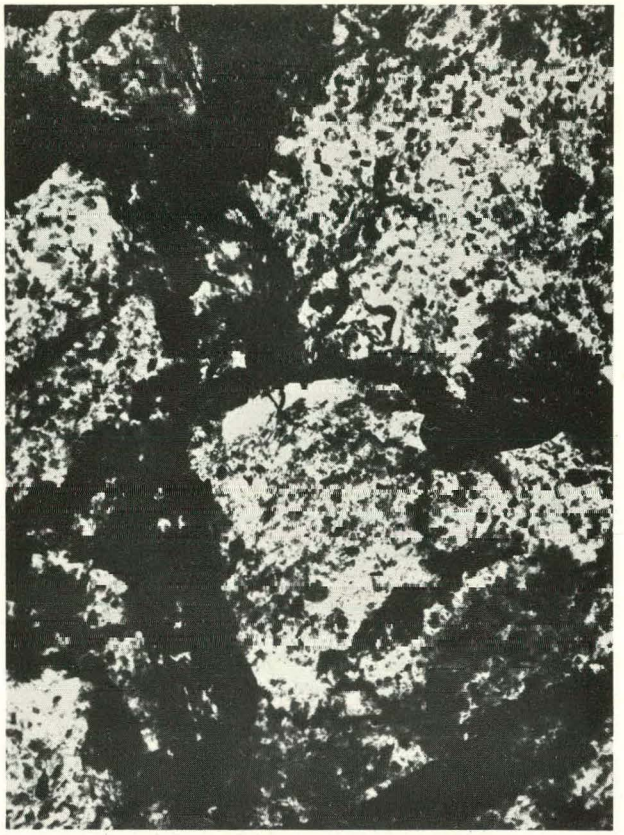

Figure A-8 6000X

Extraction Replica From Tube
Surface. Corrosion Product
From Plated-Out Area

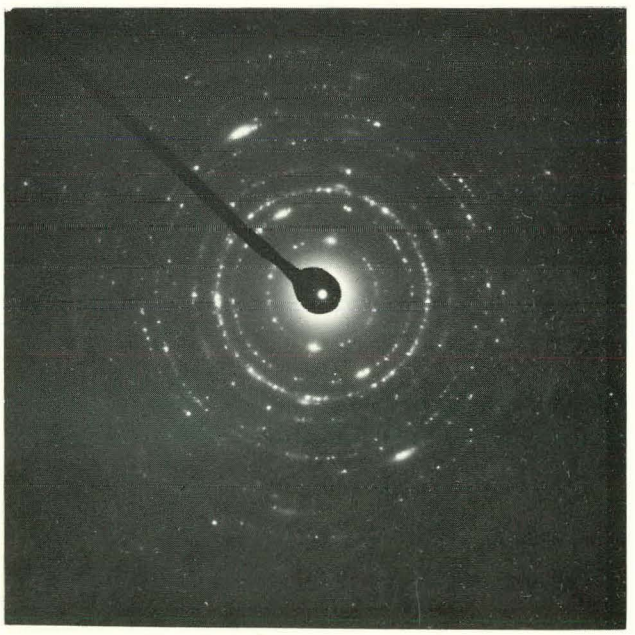

Electron Diffraction Pattern
Of Area Shown In Figure A-8

Figure A-9

TABLE A-I

DIFFRACTION DATA FOR FIGURE A-9

Camera Constant $\lambda L = 22.45$ Å mm

Radius r of rings (mm)	Spacing $d = \frac{\lambda L}{r}$ (Å)	(hkl)	Lattice Parameter $a = d_{hkl}\sqrt{h^2 + k^2 + l^2}$
4.65	4.83	111	8.36
5.30	4.24	200	8.48
7.53	2.98	220	8.43
8.75	2.57	311	8.52
9.28	2.42	222	8.38
10.75	2.09	400	8.36
11.85	1.90	331	
12.57	1.79	420	
13.08	1.72	422	
13.81	1.63	333,511	
15.10	1.49	440	

Lattice parameter approx. 8.4 Å

DISTRIBUTION LIST

	No. of Copies
C. A. Pursel, Dir. Reactor Engineering Div. Chicago Operations Office U. S. Atomic Energy Commission 9800 South Cass Avenue Argonne, Illinois	3
W. H. Brummett, Jr., Dir. Contracts Division U. S. Atomic Energy Commission San Francisco Operations Office 2111 Bancroft Way Berkeley 4, California	3
Dr. J. M. West General Nuclear Engineering Corp. P. O. Box 245 Dunedin, Florida	2
Gunnar Johnson Nuclear Power Dept. - Greendale P. O. Box 512 Milwaukee 1, Wisconsin	2
Dr. A. V. Crewe Argonne National Laboratory P. O. Box 299 Lemont, Illinois	2
Arthur F. Miller Business Manager Combustion Engineering, Inc. Nuclear Division Windsor, Connecticut	2
E. C. Ward Northern States Power Company Minneapolis, Minnesota	2
J. Wright Atomic Power Department Westinghouse Electric Corporation P. O. Box 355 Pittsburgh 30, Pennsylvania	2
Jules Wise U. S. Atomic Energy Commission New York Operations Office 376 Hudson Street New York 14, N. Y.	1
W. R. Voigt Chief, Water Reactors Branch U. S. Atomic Energy Commission Washington 25, D. C.	1

DISTRIBUTION LIST (Continued)

	No. of Copies
D. F. Cope Director, Reactor Division Oak Ridge Operations Office U. S. Atomic Energy Commission P. O. Box E Oak Ridge, Tennessee	1
W. S. Dowis Hanford Atomic Products Operation Irradiation Processing Department General Electric Company Richland, Washington	1
Division of Technical Information Extension U. S. Atomic Energy Commission P. O. Box 62 Oak Ridge, Tennessee	3 and repros